



Planet signatures in transition disks



Wladimir Lyra

California State University
Jet Propulsion Laboratory

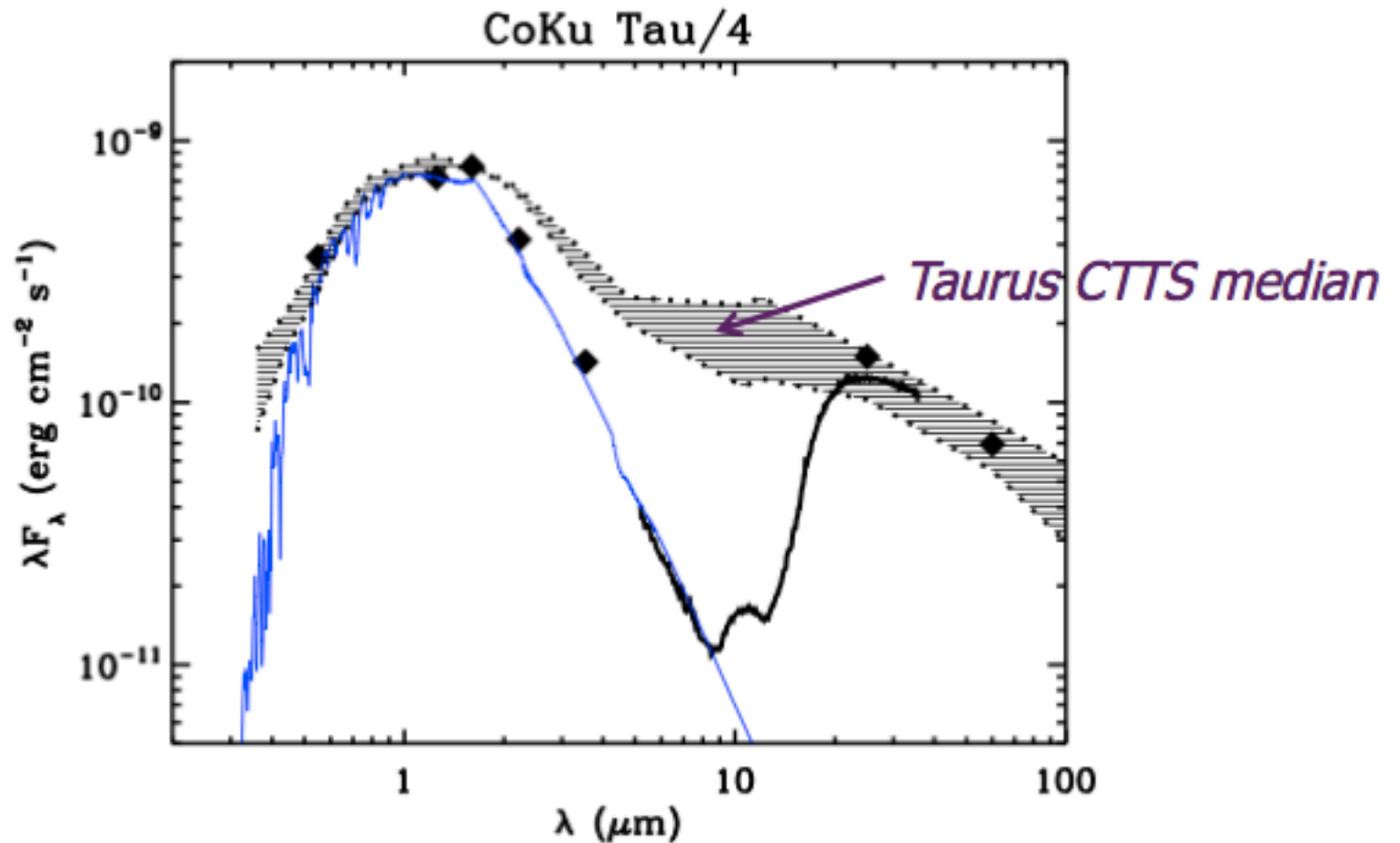
Collaborators

Aaron Boley (Vancouver), Axel Brandenburg (Stockholm),
Kees Dullemond (Heidelberg), Mario Flock (JPL), Blake Hord (New York)
Anders Johansen (Lund), Tobias Heinemann (KITP), Hubert Klahr
(Heidelberg), Marc Kuchner (Goddard), Min-Kai Lin (ASIAA), Mordecai-Mark
Mac Low (AMNH), Colin McNally (Copenhagen), Krzysztof Mizerski
(Warsaw), Richard Nelson (London) Satoshi Okuzumi (Tokyo), Sijme-Jan
Paardekooper (London), Nikolai Piskunov (Uppsala), Natalie Raettig
(Heidelberg), b, Zsolt Sandor (Budapest) Neal Turner (NASA JPL), Orkan
Umurhan (NASA Ames), Miguel de Val-Borro (NASA Goddard), Nienke van
der Marel (IfA Hawaii), Andras Zsom (Brown).

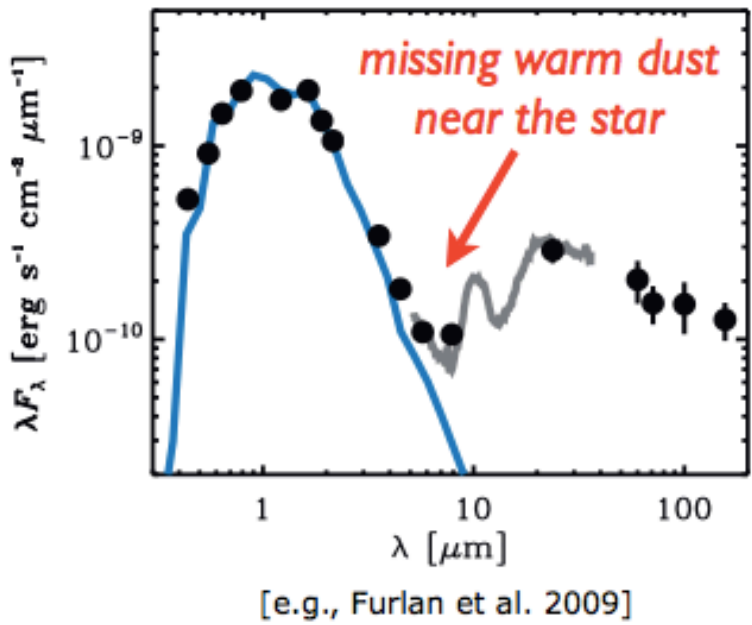


Lund, Aug 22nd, 2018

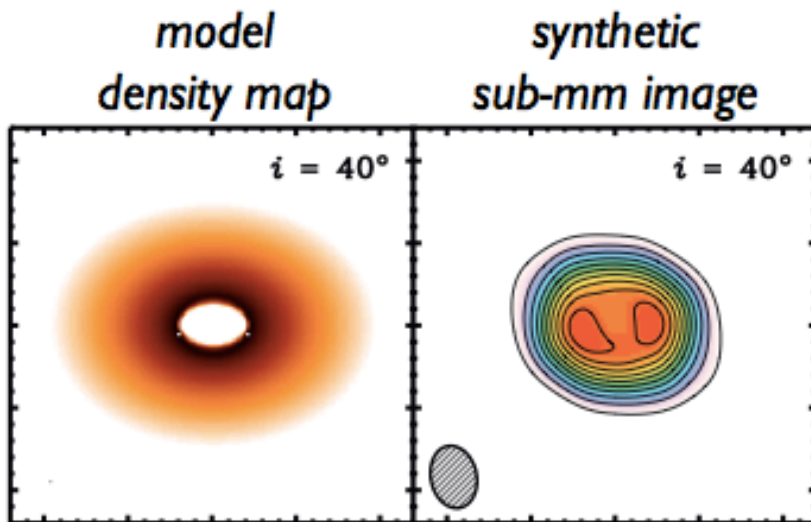
Transition Disks: Disks with missing hot dust.



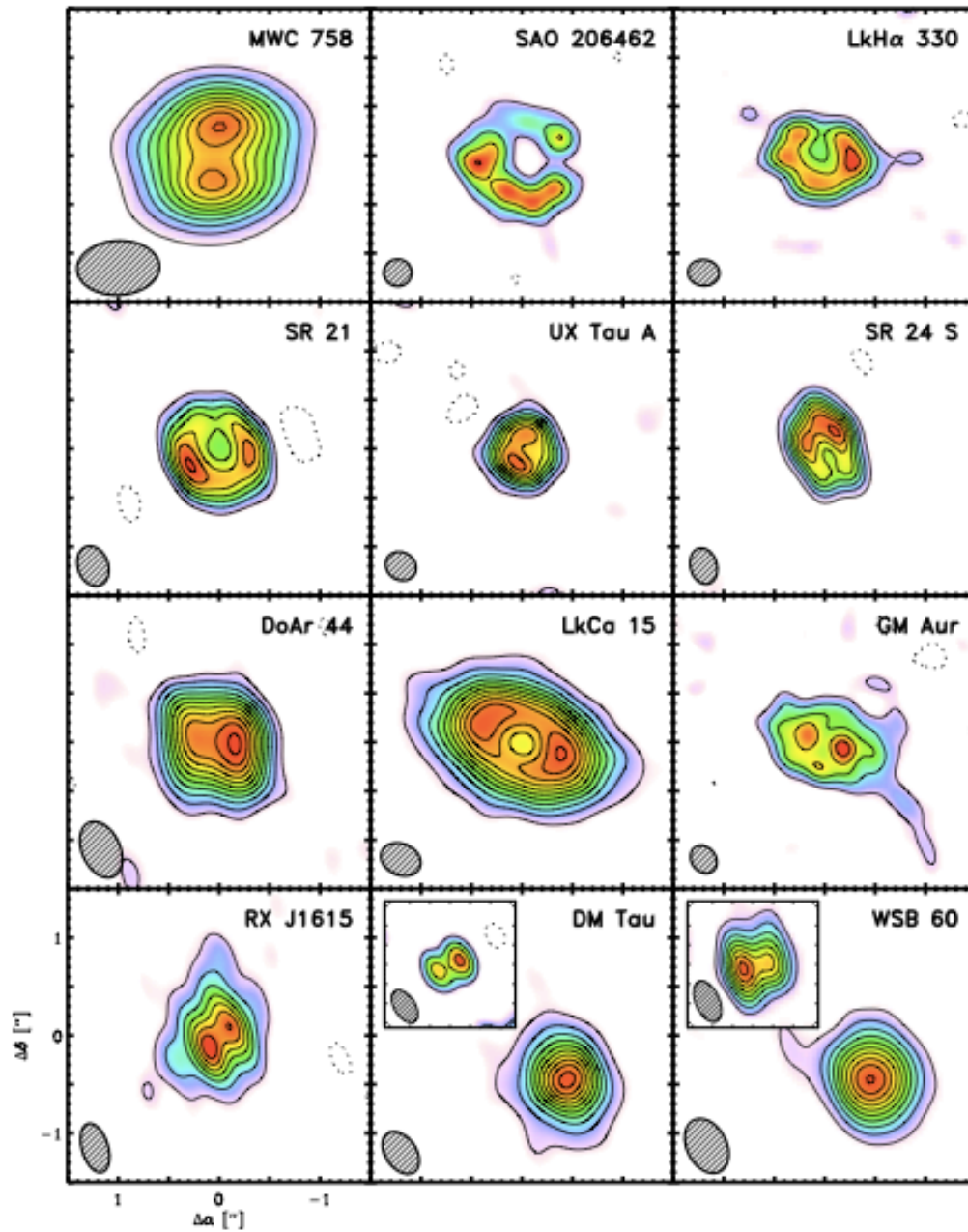
Transition Disks: Disks with missing hot dust.



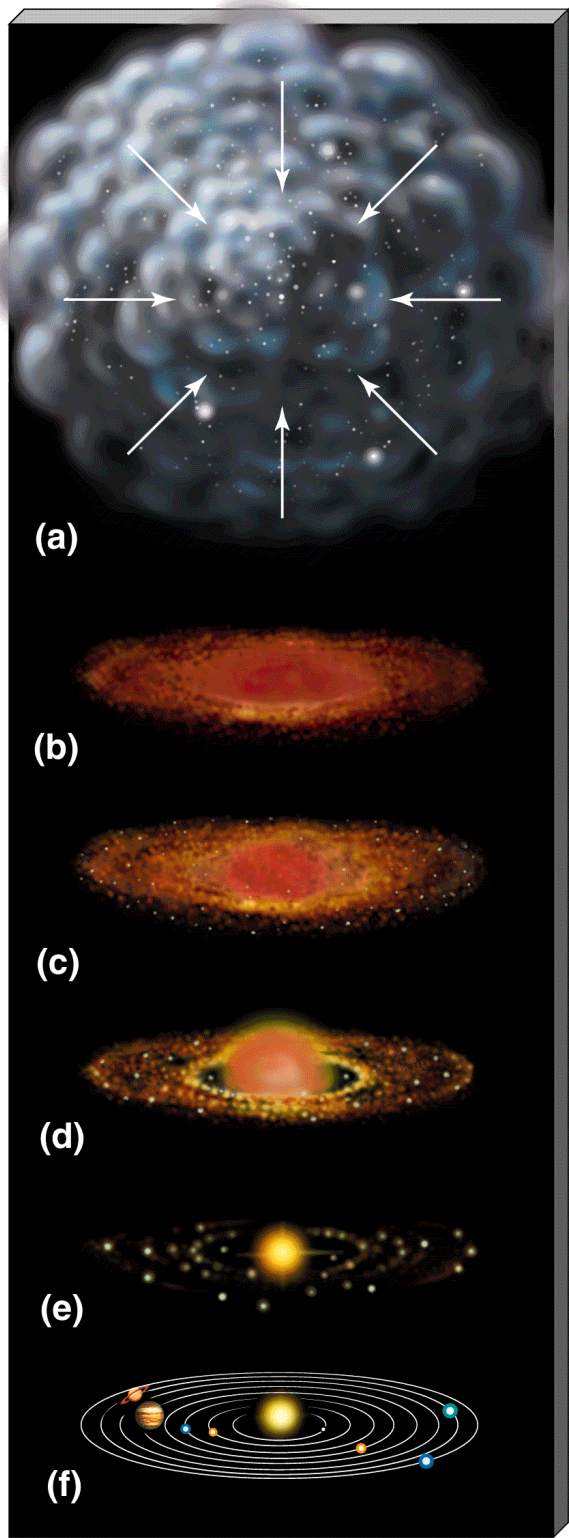
a disk with a large reduction
in optical depth near the star
(i.e., a “cavity” or “hole”)



Resolved transition disks with the Sub-millimeter Array (SMA)



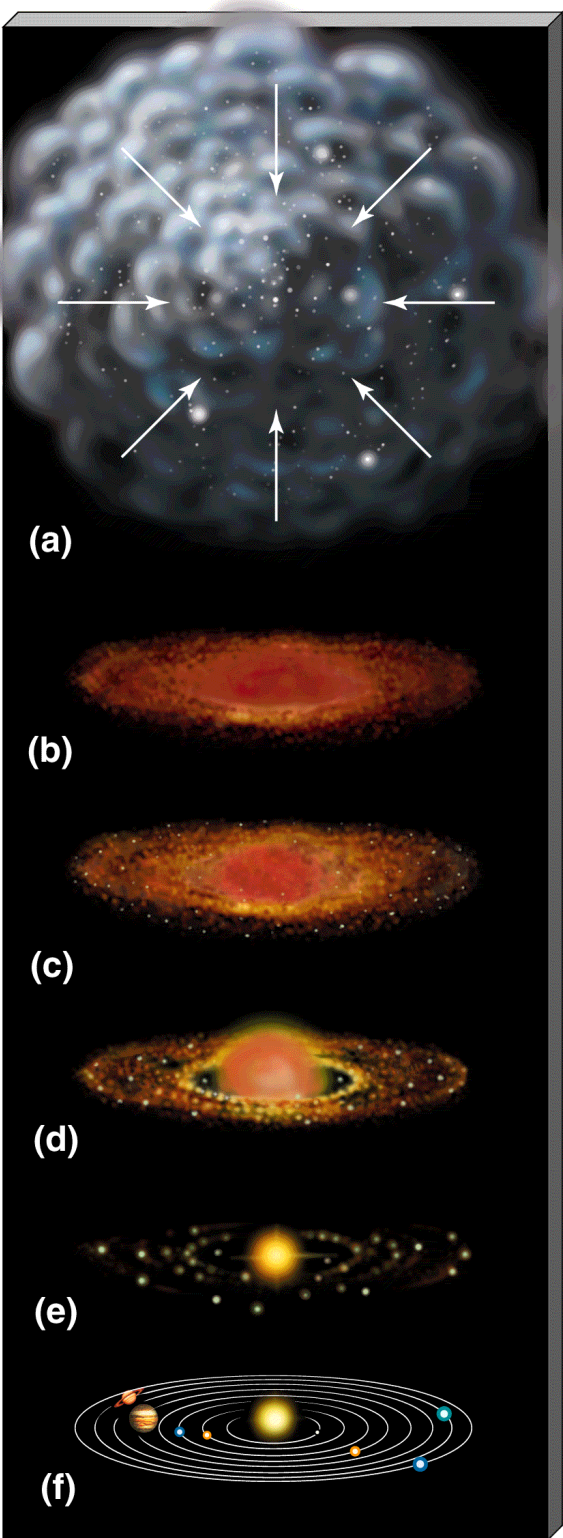
0.85mm
0.3" ~ 20 AU resolution



Are transitional disks
related to disk evolution?

Gas-rich phase (< 10 Myr)
Primordial Disks

Gas-poor phase (>10 Myr)
Debris Disks



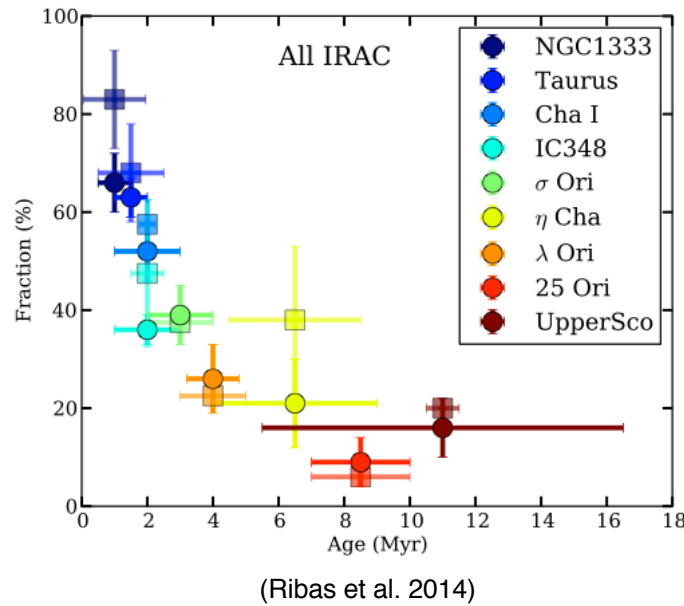
Are transitional disks
related to disk evolution?

Gas-rich phase (< 10 Myr)
Primordial Disks

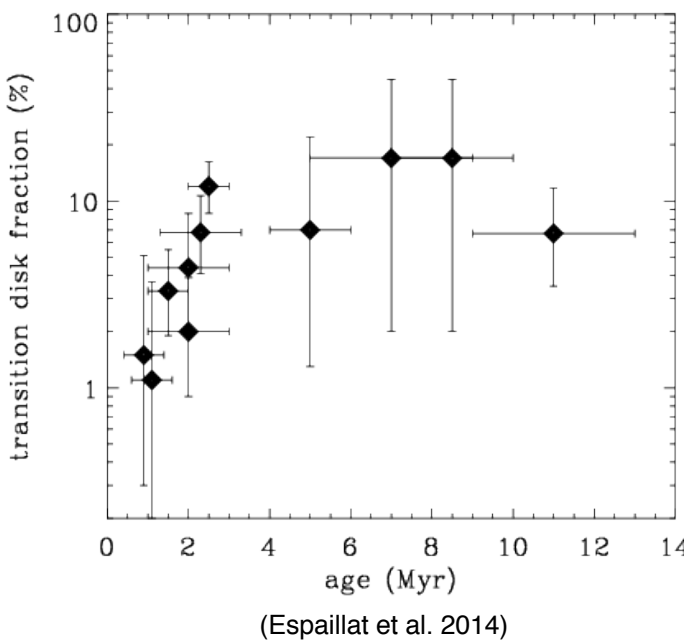
Conjecture:
Thinning phase (~10 Myr)
Transitional Disks

Gas-poor phase (>10 Myr)
Debris Disks

Transition disks and disk evolution

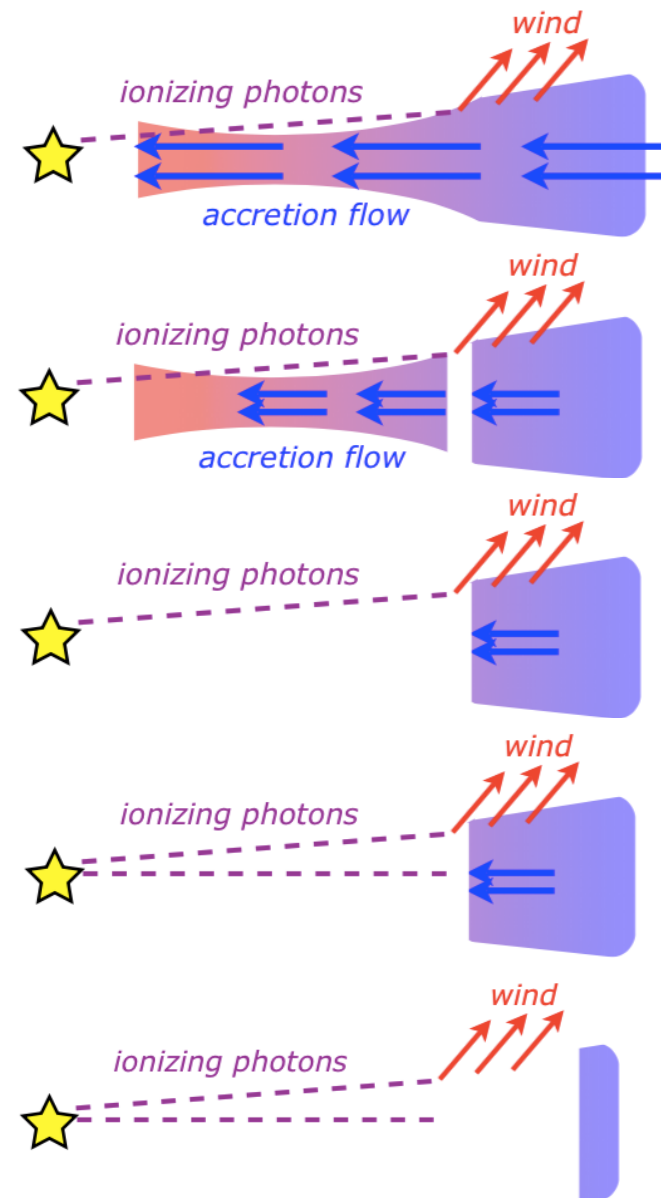


“Total” disk fraction



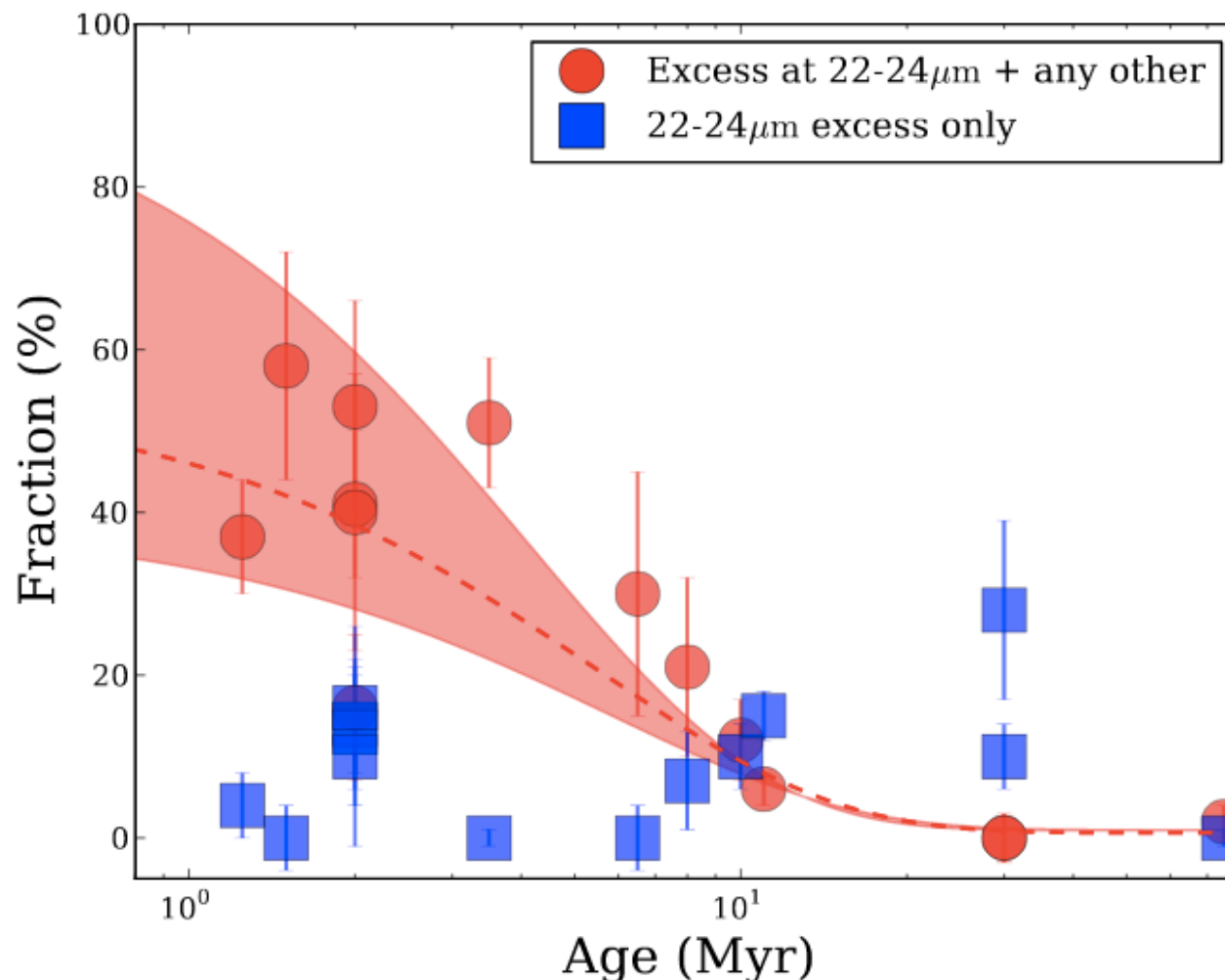
Transition disk fraction

Photoevaporation



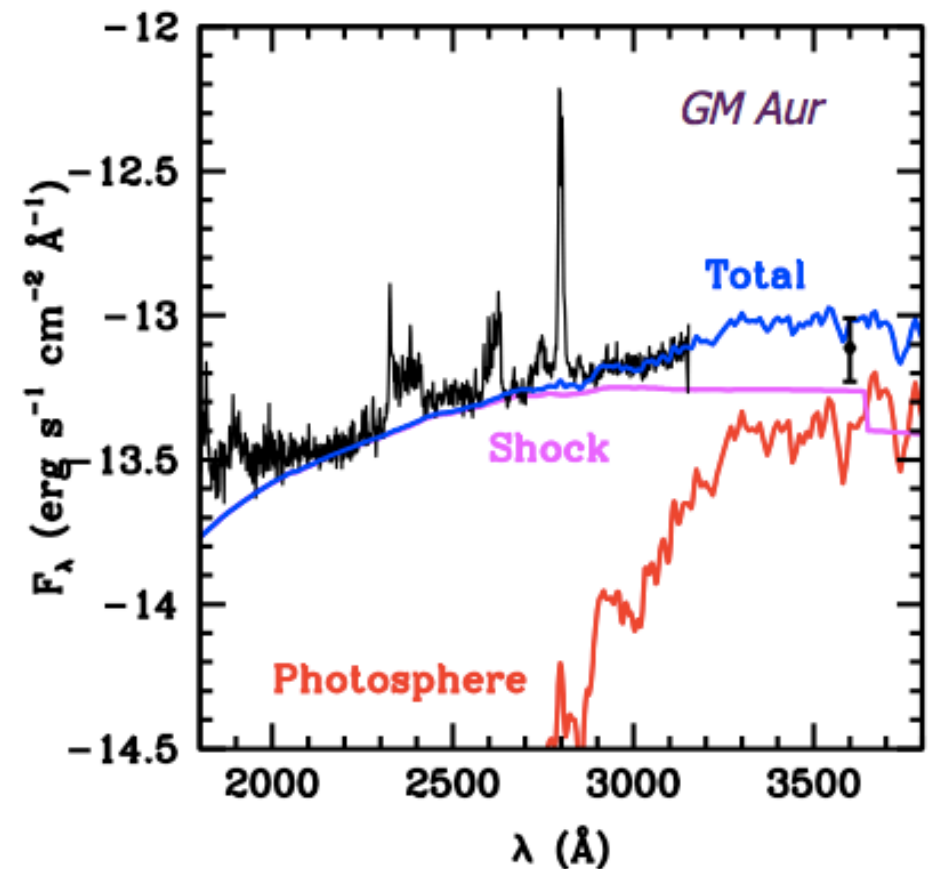
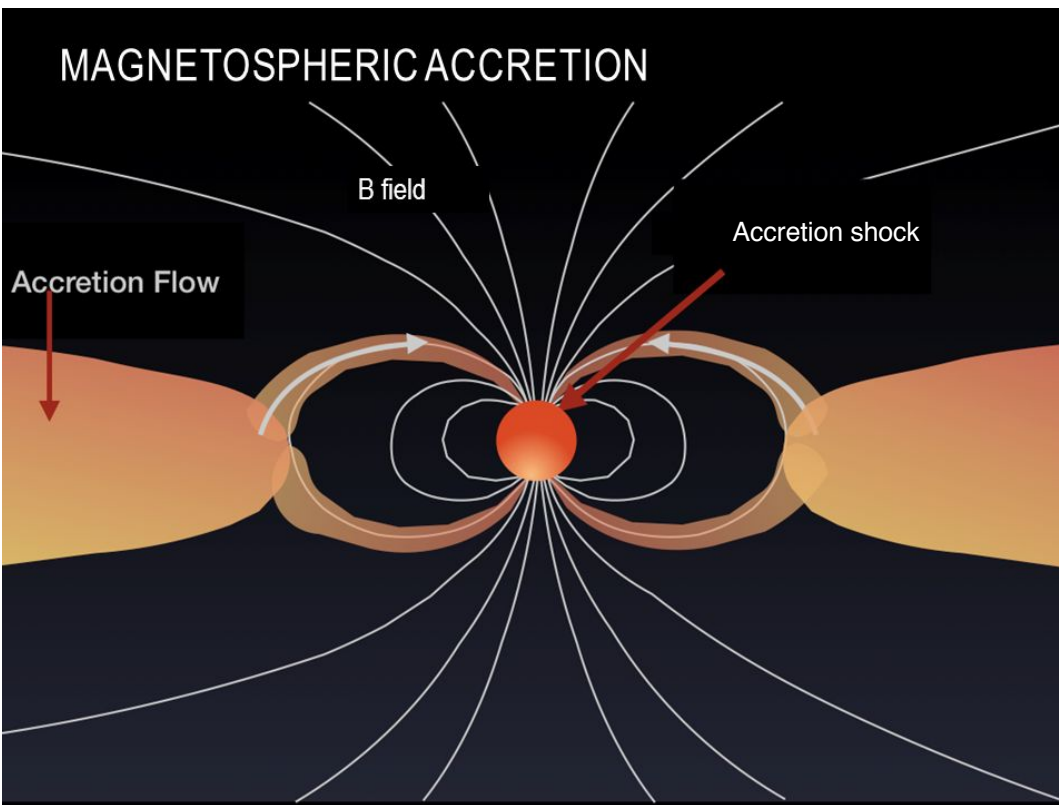
Transition disks linked to disk evolution?

The distribution in age is consistent with a uniform distribution.

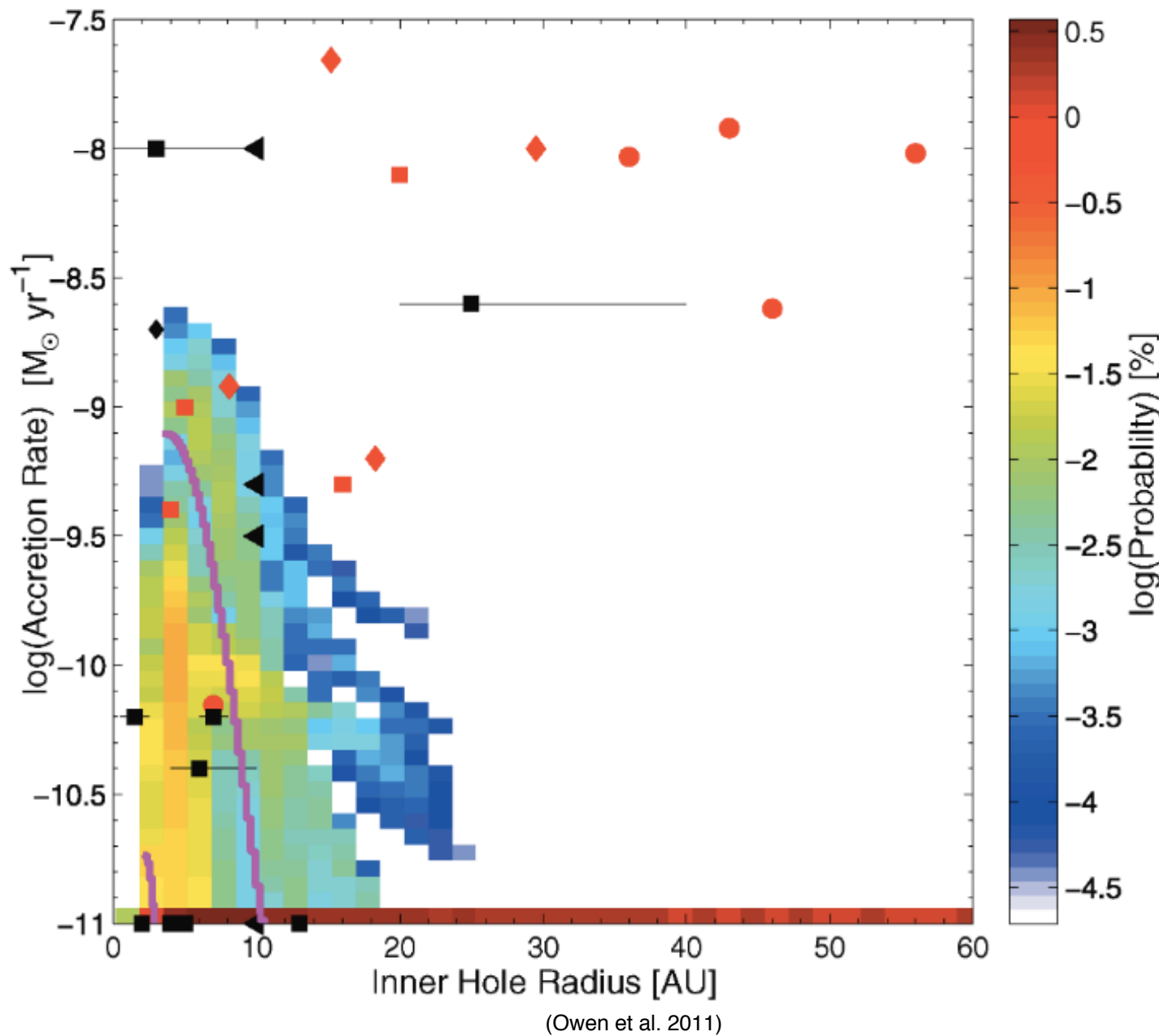


UV excess

Many transitional disks show signs of accretion, at the level of primordial (classical T-Tauri) disks.



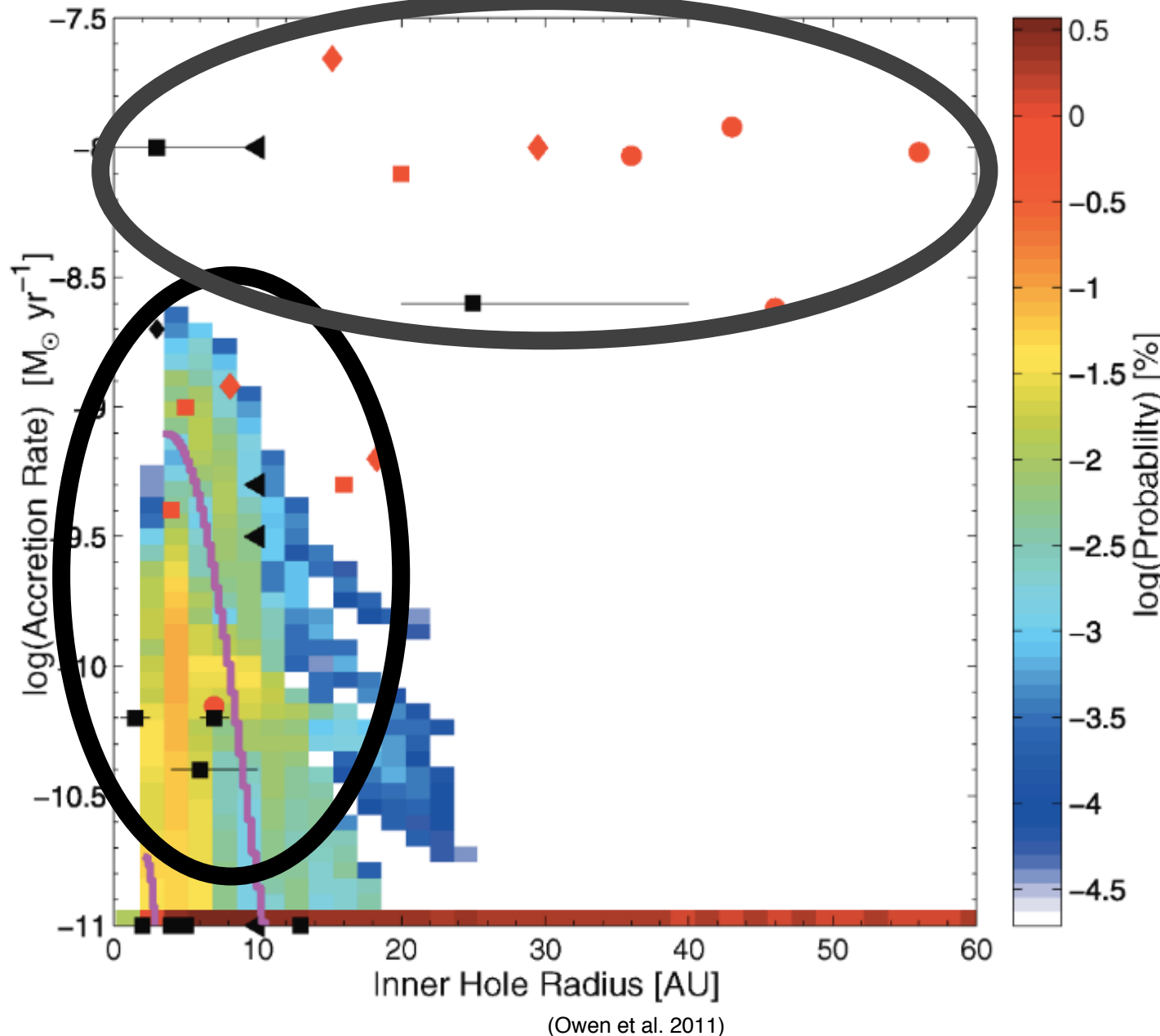
Bimodal distribution of transition disks



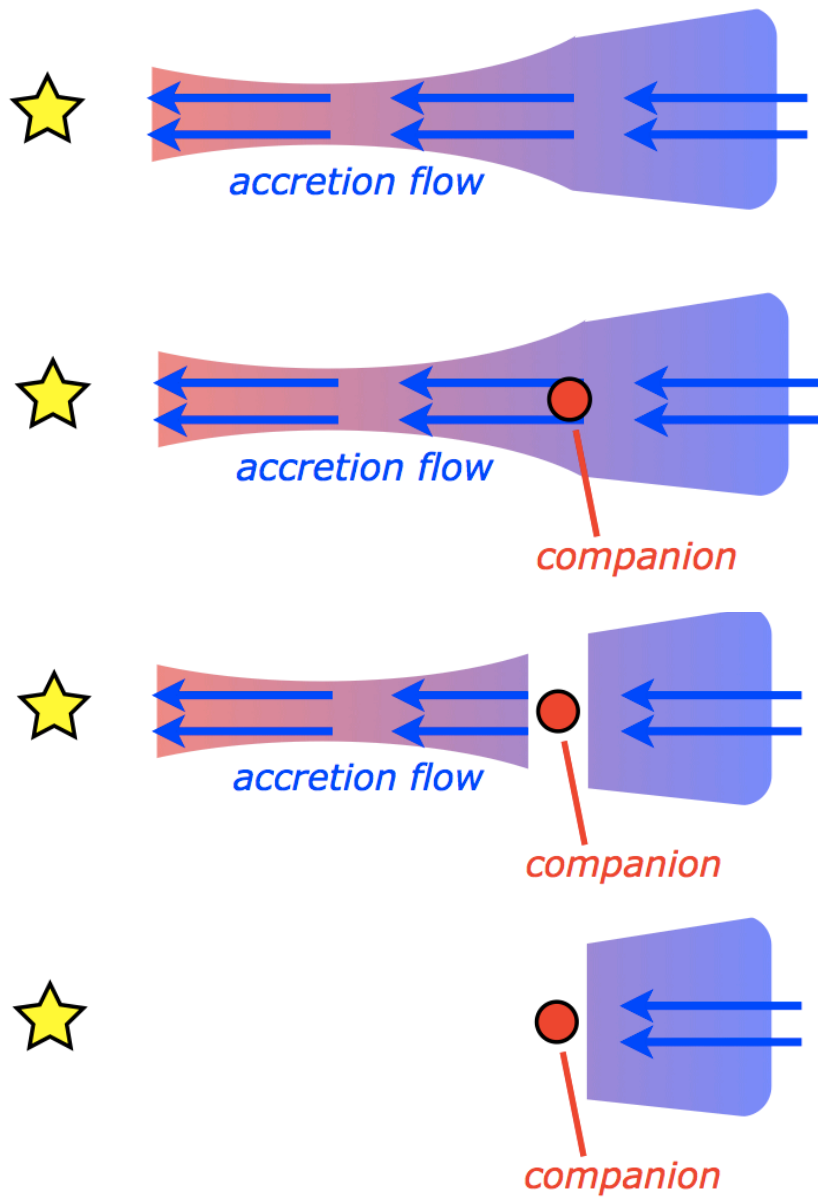
Bimodal distribution of transition disks

Not explained by photo-evaporation

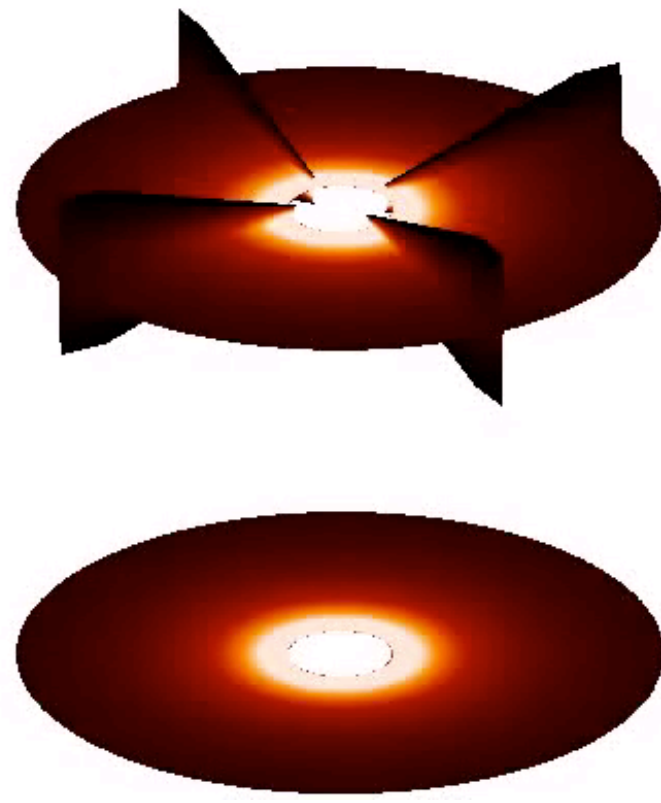
*Explained by
Photo-
evaporation*



Planetary companion

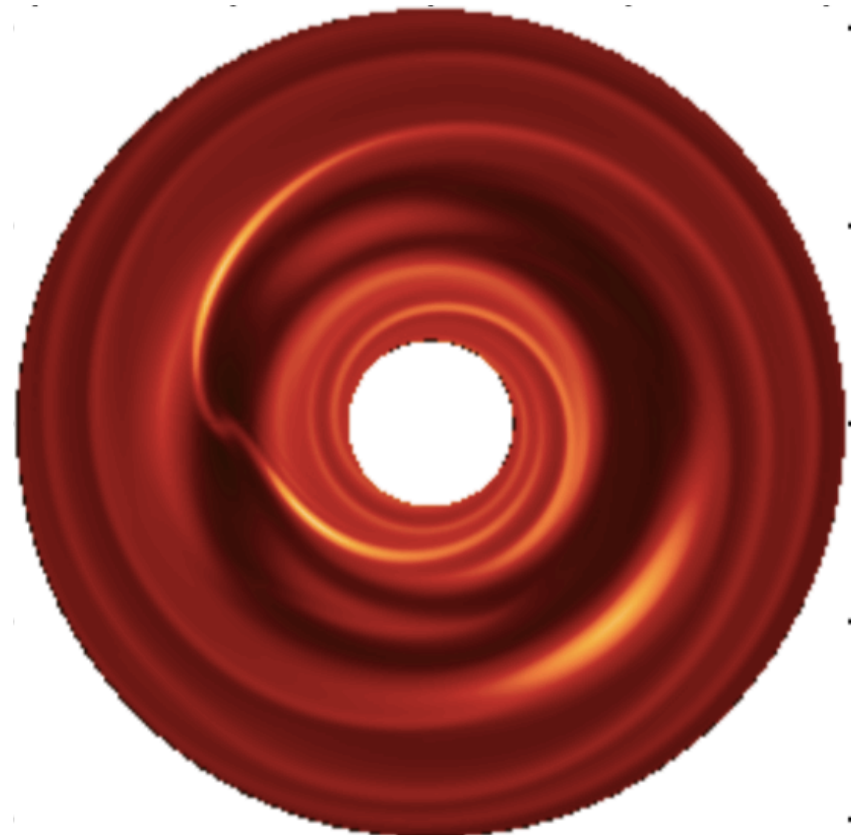
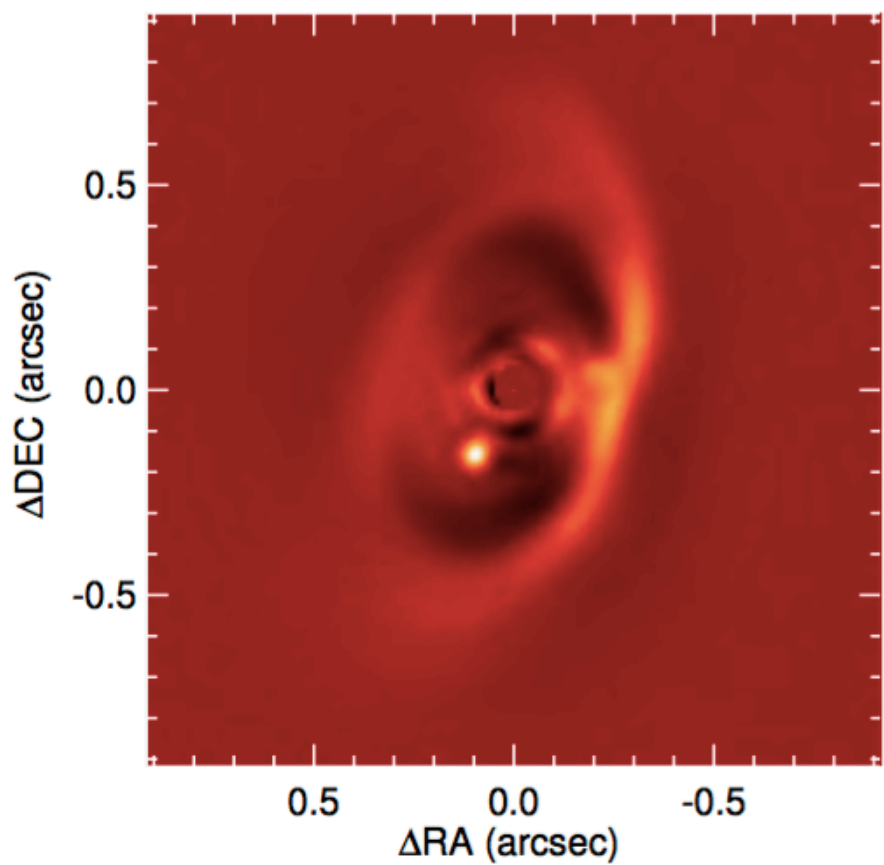


$t = 0.1$



(Lyra 2009)

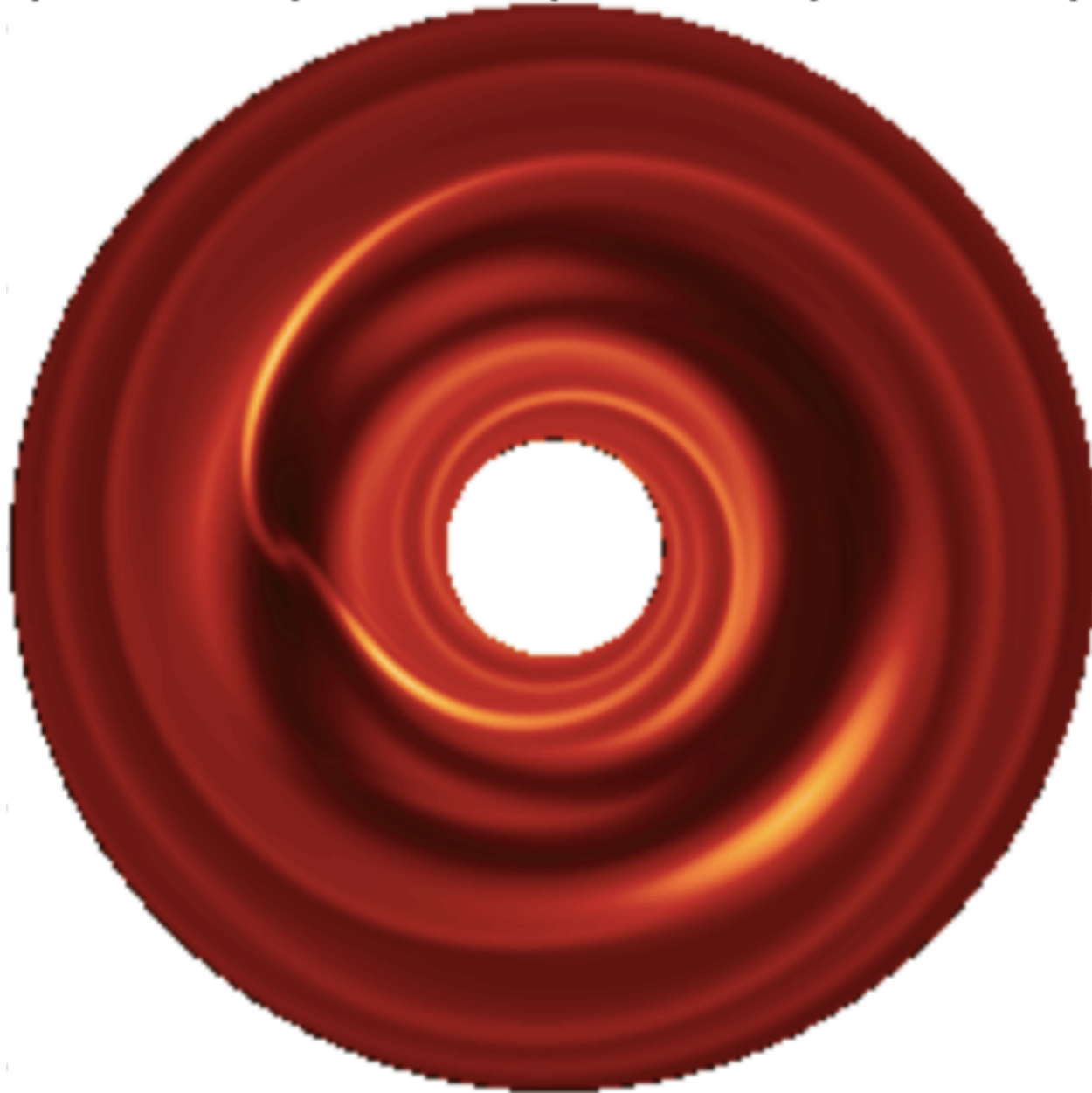
These cavities may be the telltale signature of forming planets



(Lyra et al. 2009b)

A way to directly study planet-disk interaction

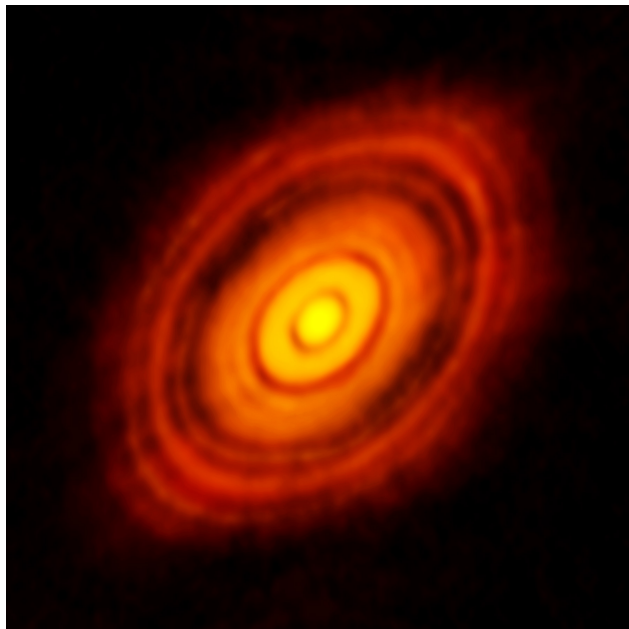
Planet-disk interaction: gaps, spirals, and vortices.



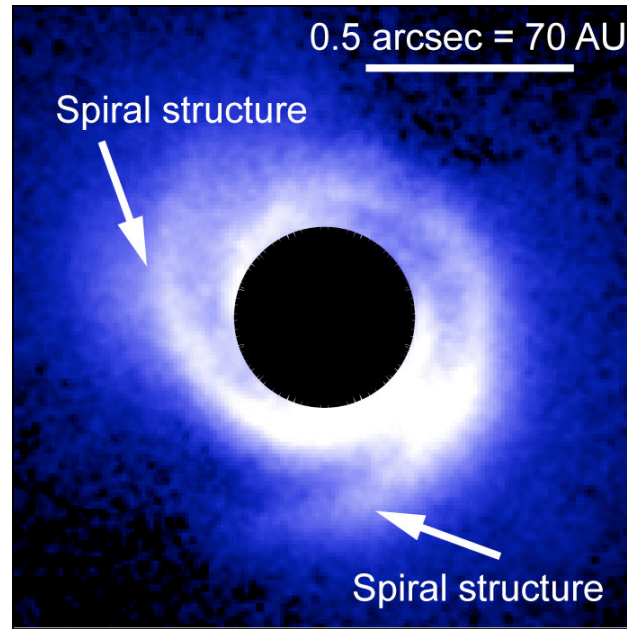
(Lyra et al. 2009b)

Observational evidence: gaps, spirals, and vortices

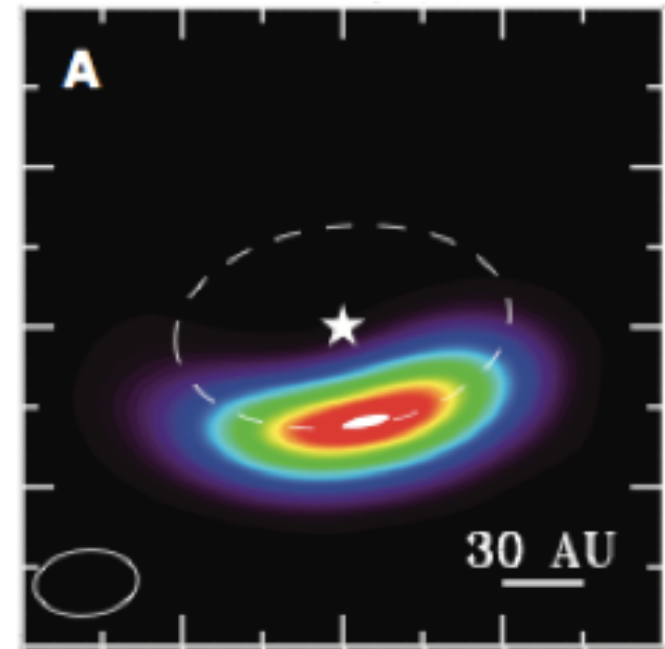
HL Tau



SAO 206462



Oph IRS 48



The ALMA Partnership et al. (2015)

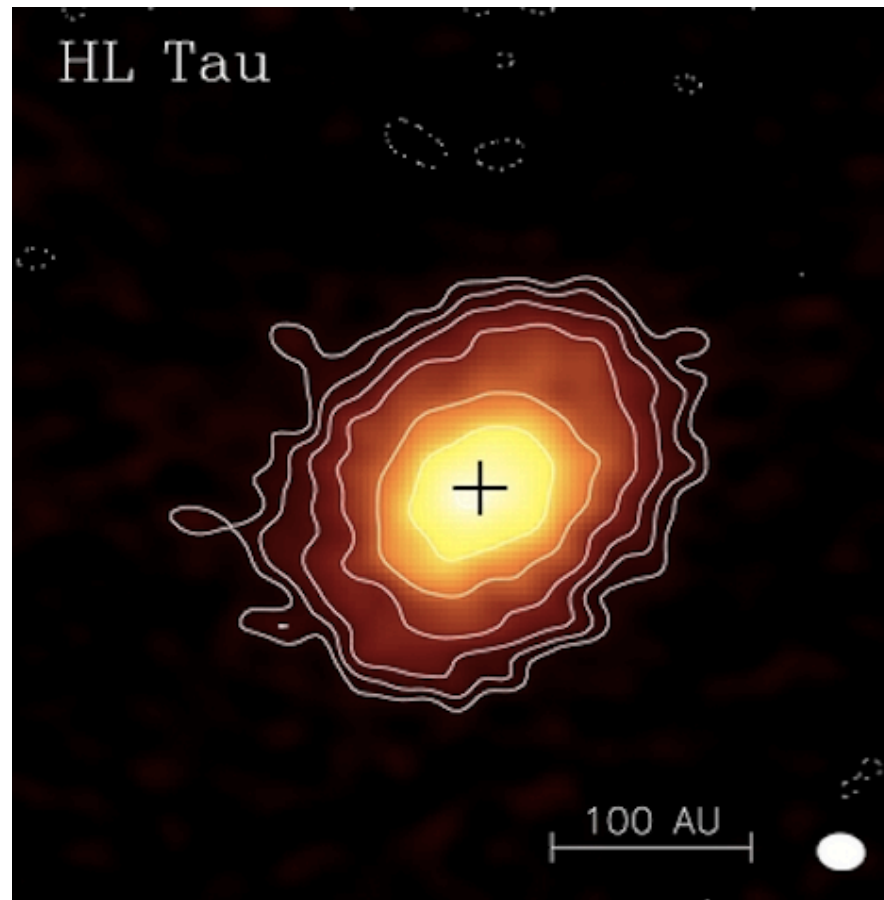
Muto et al. (2012)

van der Marel et al. (2013)

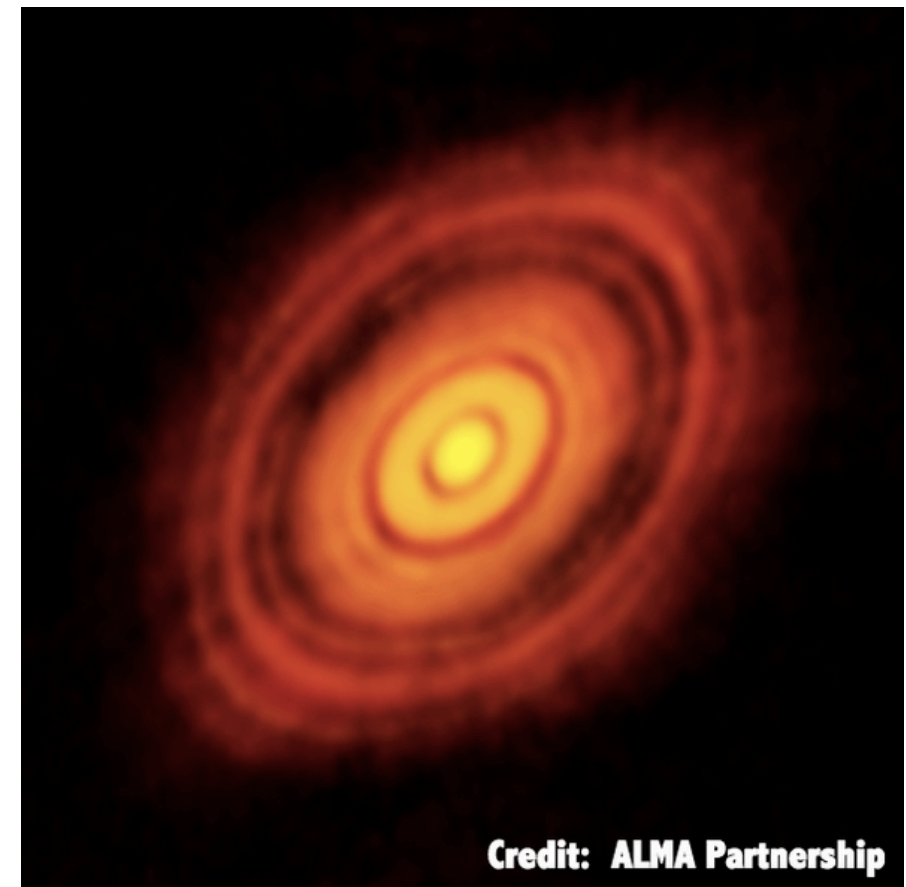
The Atacama Large Millimeter Array (ALMA)



Before ALMA

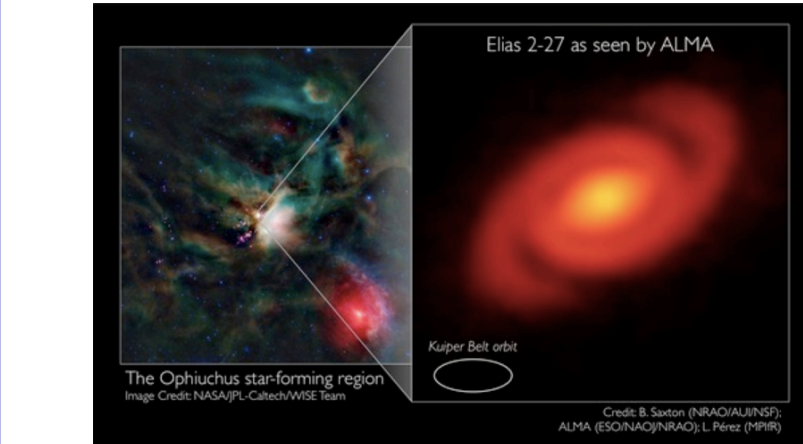


ALMA

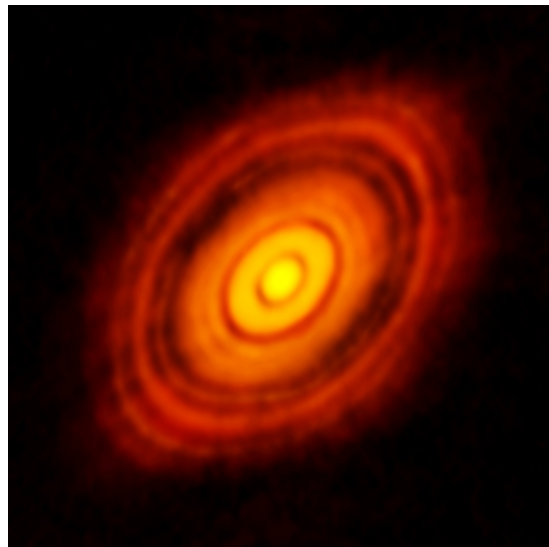


The ALMA view of Protoplanetary Disks

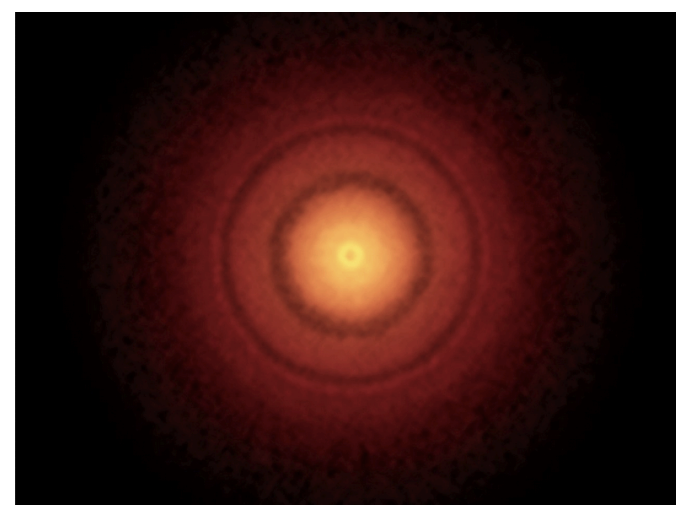
Elias 2-27



HL Tau



TW Hya



Oph IRS 48

down



A Major Asymmetric Dust Trap in a Transition Disk

Nienke van der Marel,^{1,*} Ewine F. van Dishoeck,^{1,2} Simon Bruderer,² Til Birnstiel,³ Paola Pinilla,⁴ Cornelis P. Dullemond,⁴ Tim A. van Kempen,^{1,5} Markus Schmalzl,¹ Joanna M. Brown,³ Gregory J. Herczeg,⁶ Geoffrey S. Mathews,¹ Vincent Geers⁷

The statistics of discovered exoplanets suggest that planets form efficiently. However, there are fundamental unsolved problems, such as excessive inward drift of particles in protoplanetary disks during planet formation. Recent theories invoke dust traps to overcome this problem. We report the detection of a dust trap in the disk around the star Oph IRS 48 using observations from the Atacama Large Millimeter/submillimeter Array (ALMA). The 0.44-millimeter-wavelength continuum map shows high-contrast crescent-shaped emission on one side of the star, originating from millimeter-sized grains, whereas both the mid-infrared image (micrometer-sized dust) and the gas traced by the carbon monoxide 6-5 rotational line suggest rings centered on the star. The difference in distribution of big grains versus small grains/gas can be modeled with a vortex-shaped dust trap triggered by a companion.

Although the ubiquity of planets is confirmed almost daily by detections of new exoplanets (*1*), the exact forma-

tion mechanism of planetary systems in disks of gas and dust around young stars remains a long-standing problem in astrophysics (*2*). In

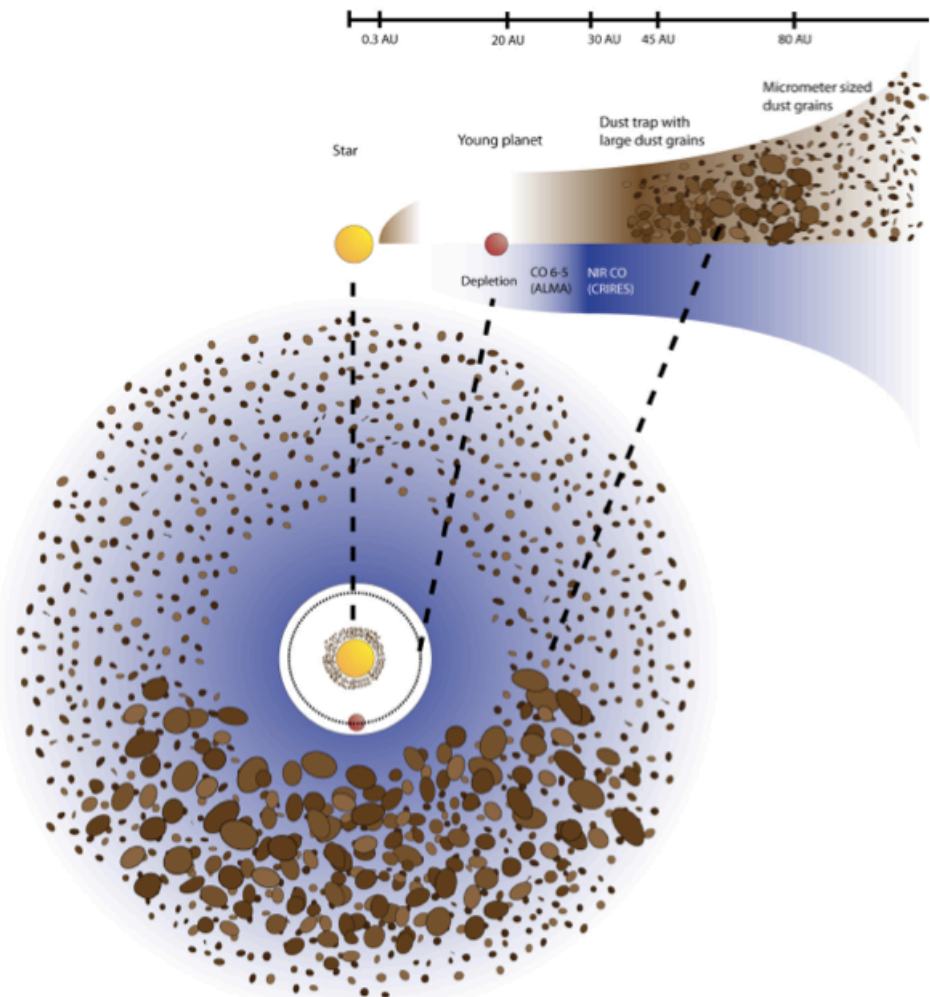
iencemag.org SCIENCE VOL 340 7 JUNE 2013

1199

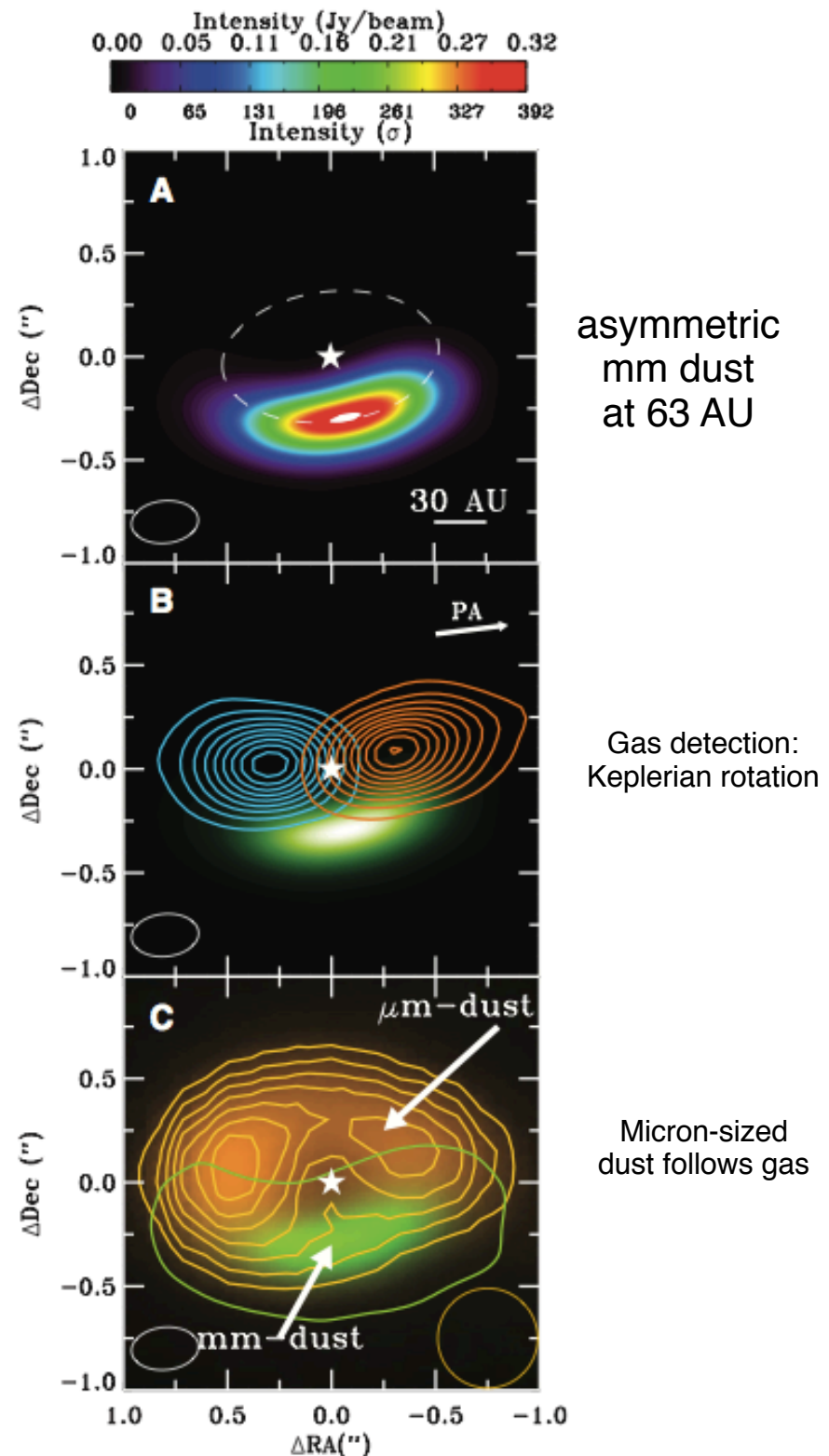
van der Marel et al. 2013

A huge vortex observed with ALMA

The Oph IRS 48 “comet formation factory”

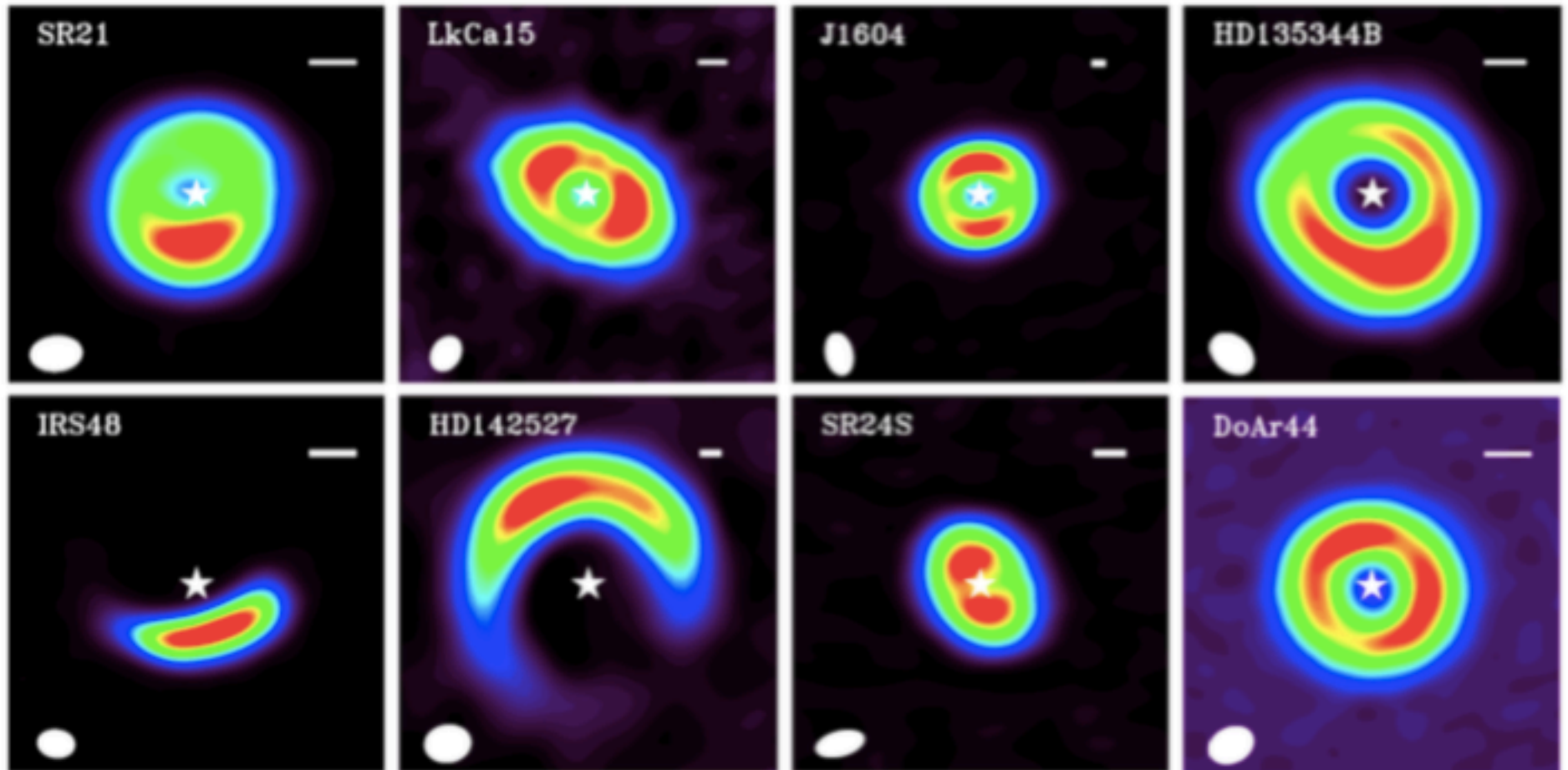


van der Marel et al. (2013)



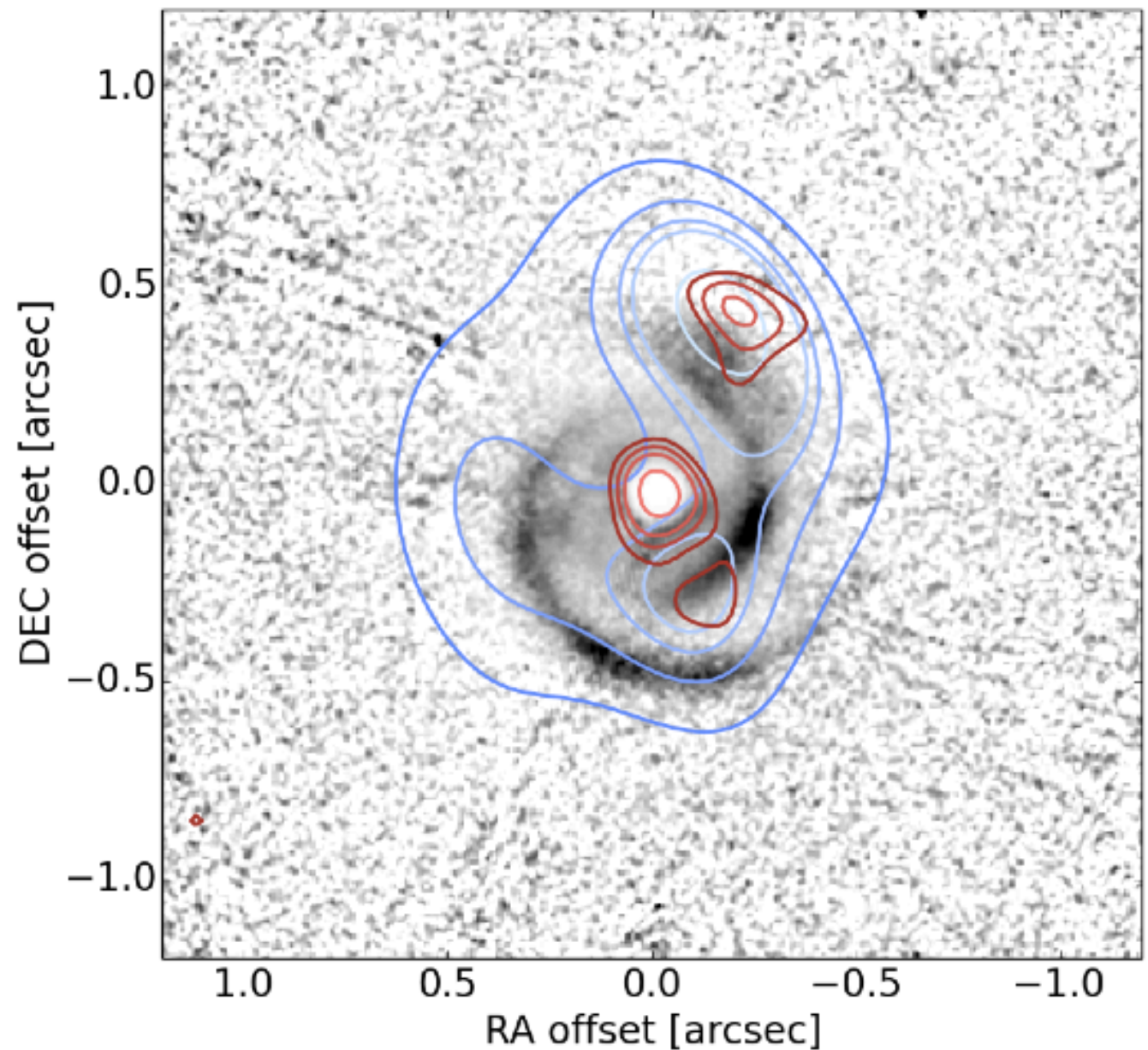
Vortices everywhere!

Extrasolar nebulae

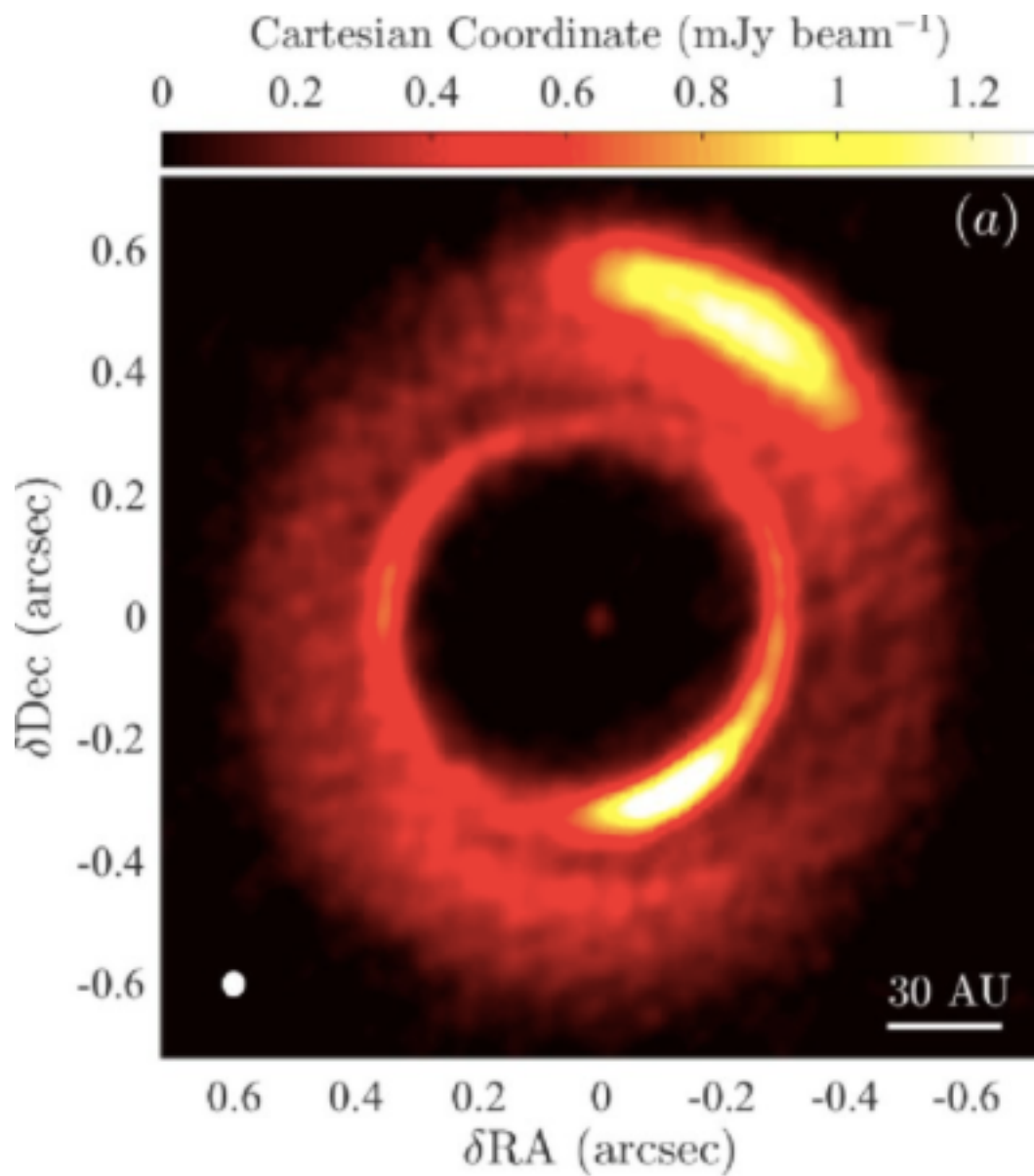


SPHERE-ALMA-VLA overlay of MWC 758

SPHERE (μm)
ALMA ($\sim \text{mm}$)
VLA (cm-m)

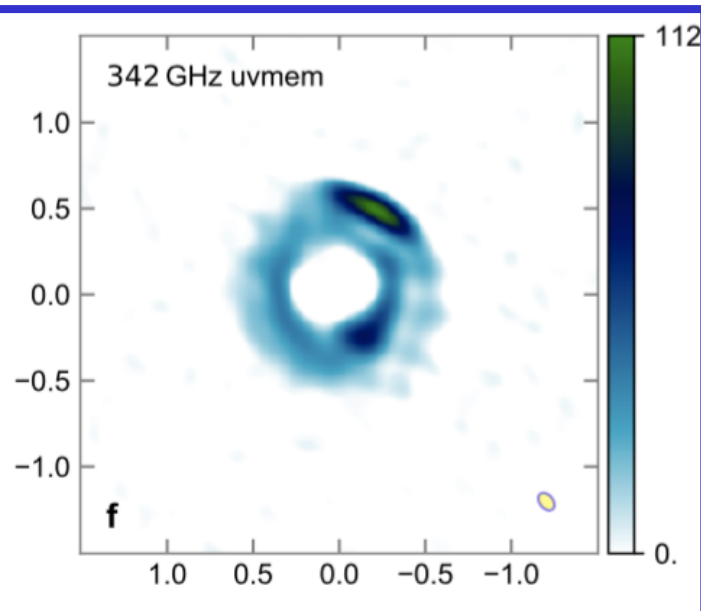


MWC 758

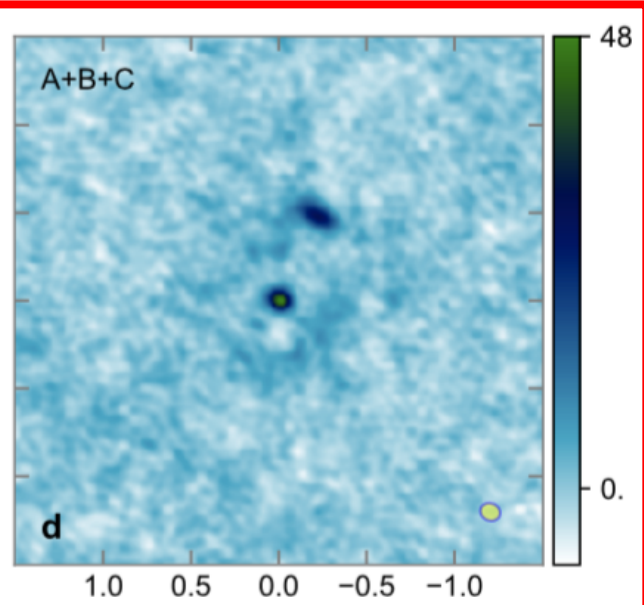


Pebble trapping

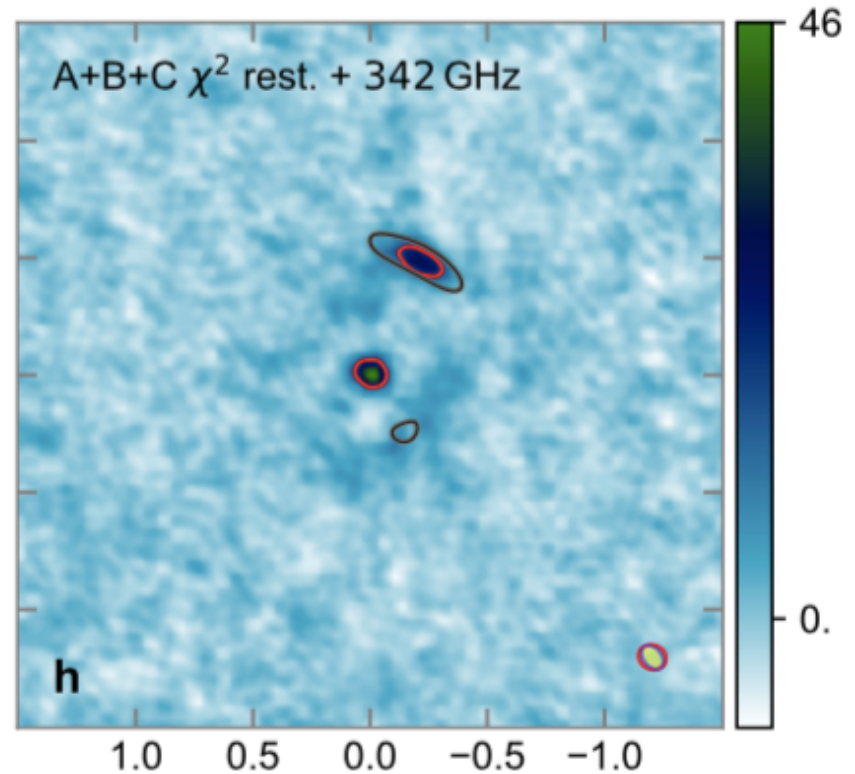
ALMA
(mm)



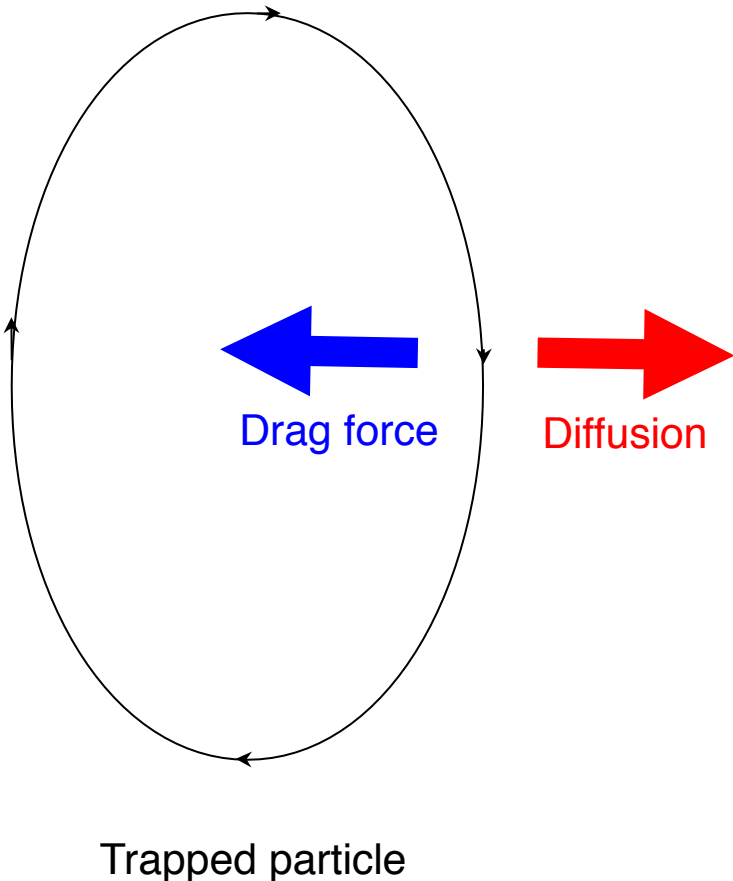
VLA
(cm-m)



Overlay



Drag-Diffusion Equilibrium



Dust continuity equation

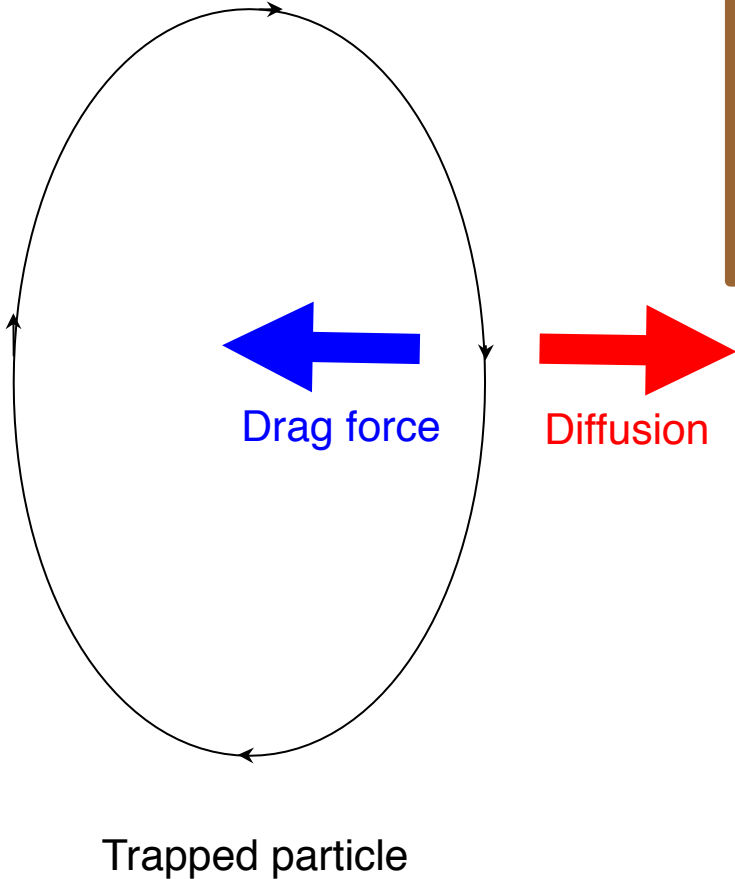
$$\frac{\partial \rho_d}{\partial t} = -(\mathbf{v} \cdot \nabla) \rho_d - \rho_d \nabla \cdot \mathbf{v} + D \nabla^2 \rho_d,$$

advection

compression

diffusion

Drag-Diffusion Equilibrium



Steady-state solution

$$\rho_d(a,z) = \epsilon \rho_0 (S + 1)^{3/2} \exp \left\{ - \frac{[a^2 f^2(\chi) + z^2]}{2H^2} (S + 1) \right\}$$

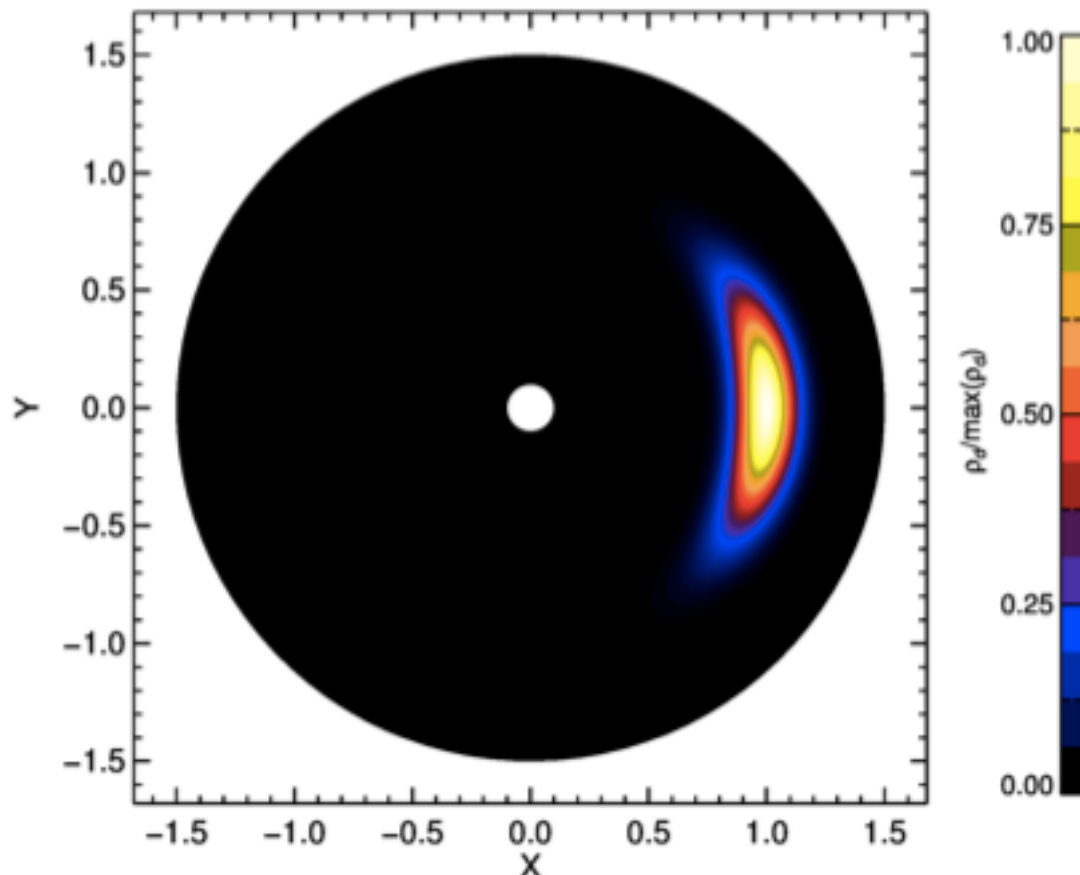
Lyra & Lin (2013)

$$S = \frac{St}{\delta}$$

$$\delta = v_{\text{rms}}^2 / c_s^2,$$

a = vortex semi-minor axis
 H = disk scale height (temperature)
 χ = vortex aspect ratio
 δ = diffusion parameter
 St = Stokes number (particle size)
 $f(\chi)$ = model-dependent scale function

Analytical solution for dust in drag-diffusion equilibrium



Solution for

$$H/r=0.1 \quad \chi=4 \quad S=1$$

Solution

$$\rho_d(a) = \rho_{d\max} \exp\left(-\frac{a^2}{2H_V^2}\right),$$

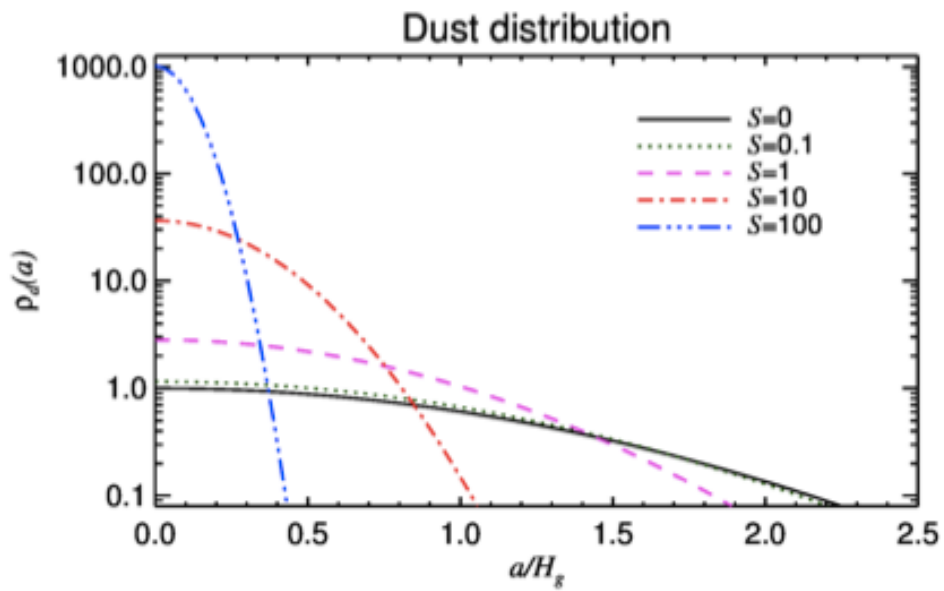
$$H_V = \frac{H}{f(\chi)} \sqrt{\frac{1}{S+1}}$$

$$S = \frac{St}{\delta}$$

$$\delta = v_{\text{rms}}^2 / c_s^2,$$

a = distance to vortex center
 H = disk scale height (temperature)
 χ = vortex aspect ratio
 δ = diffusion parameter
St = Stokes number (grain size)
 $f(\chi)$ = model-dependent scale function

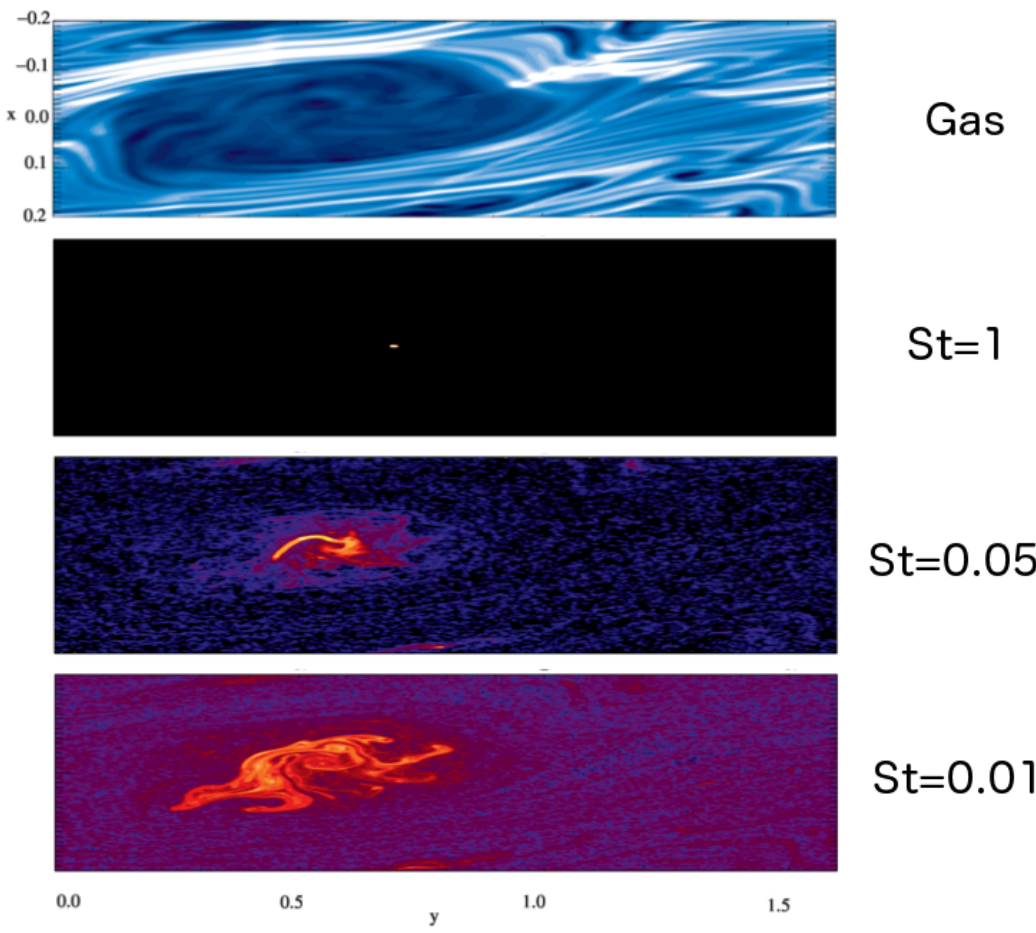
Analytical vs Numerical



$$S = \text{St}/\delta$$

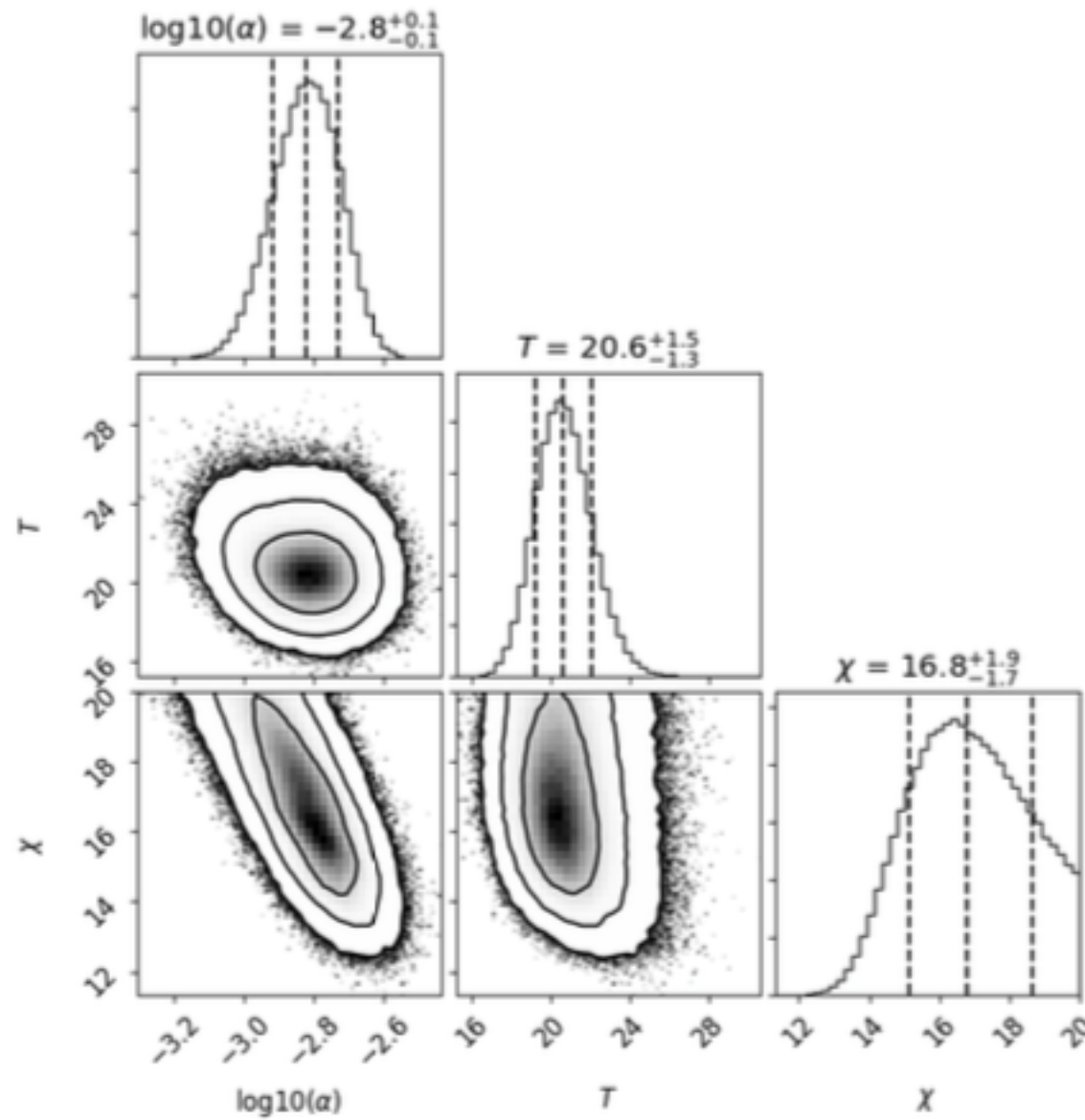
$$\delta = v_{\text{rms}}^2 / c_s^2,$$

Lyra & Lin (2013)



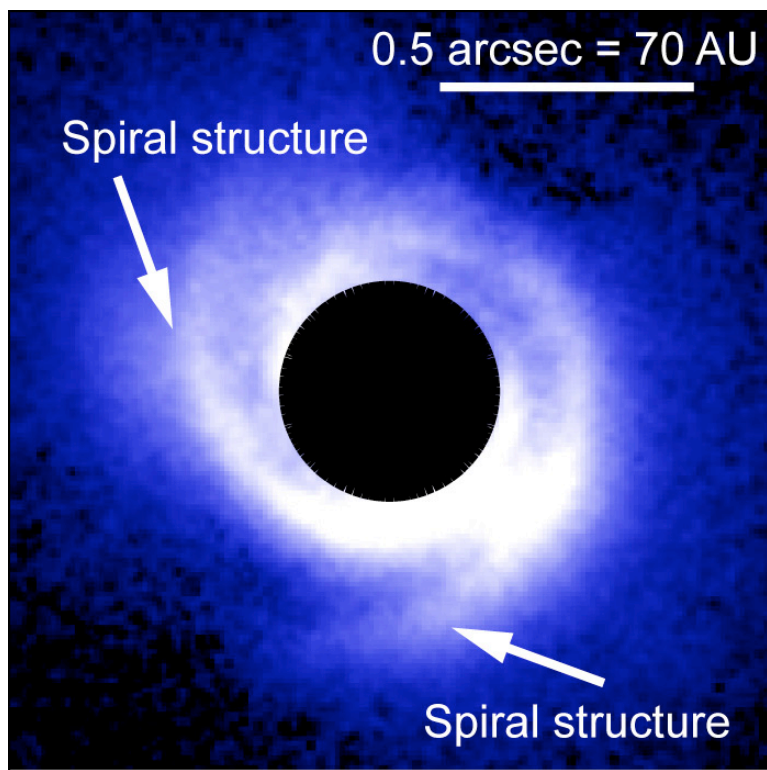
Raettig et al (2015)

Observational vs Analytical



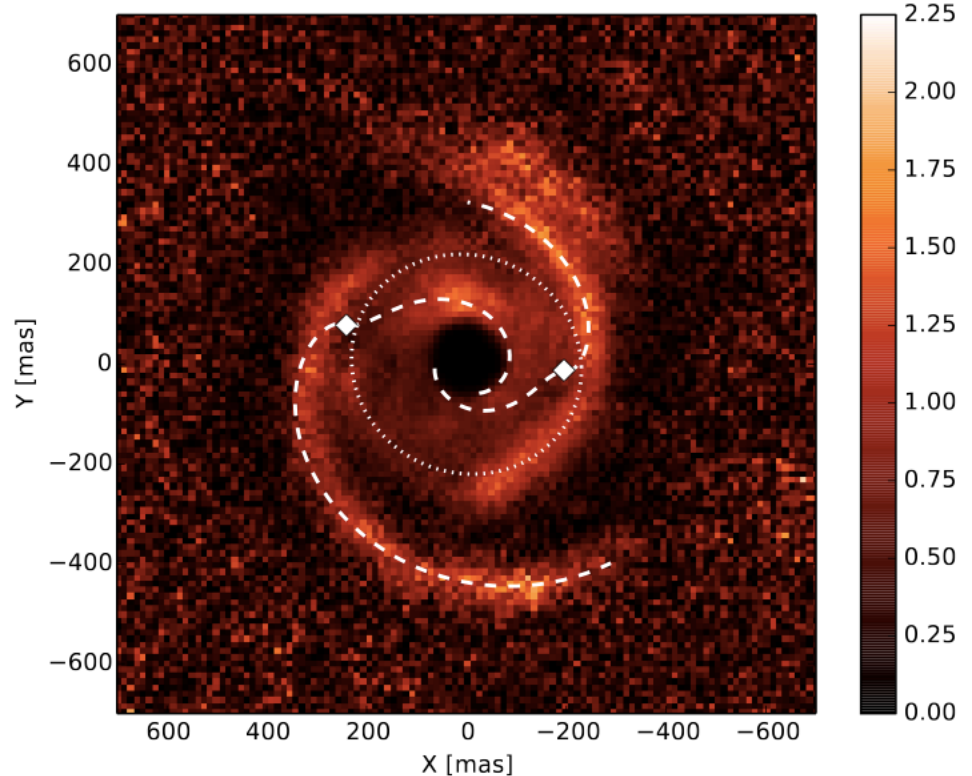
Observational Evidence: Spirals

SAO 206462



Muto et al. (2012)

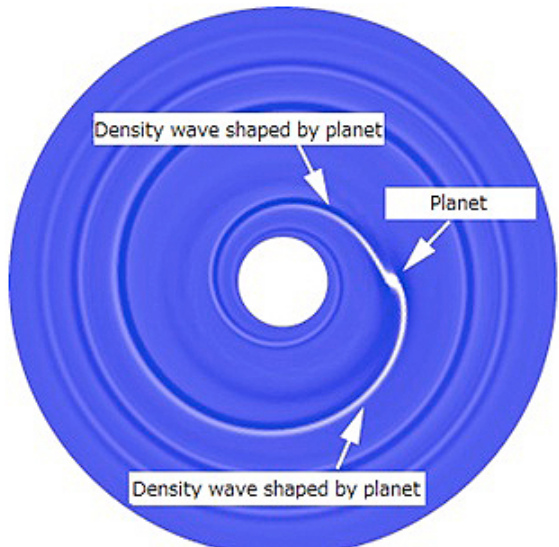
MWC 758



Benisty et al. (2015)

Spiral arm fitting leads to problems

Analytical spiral fit

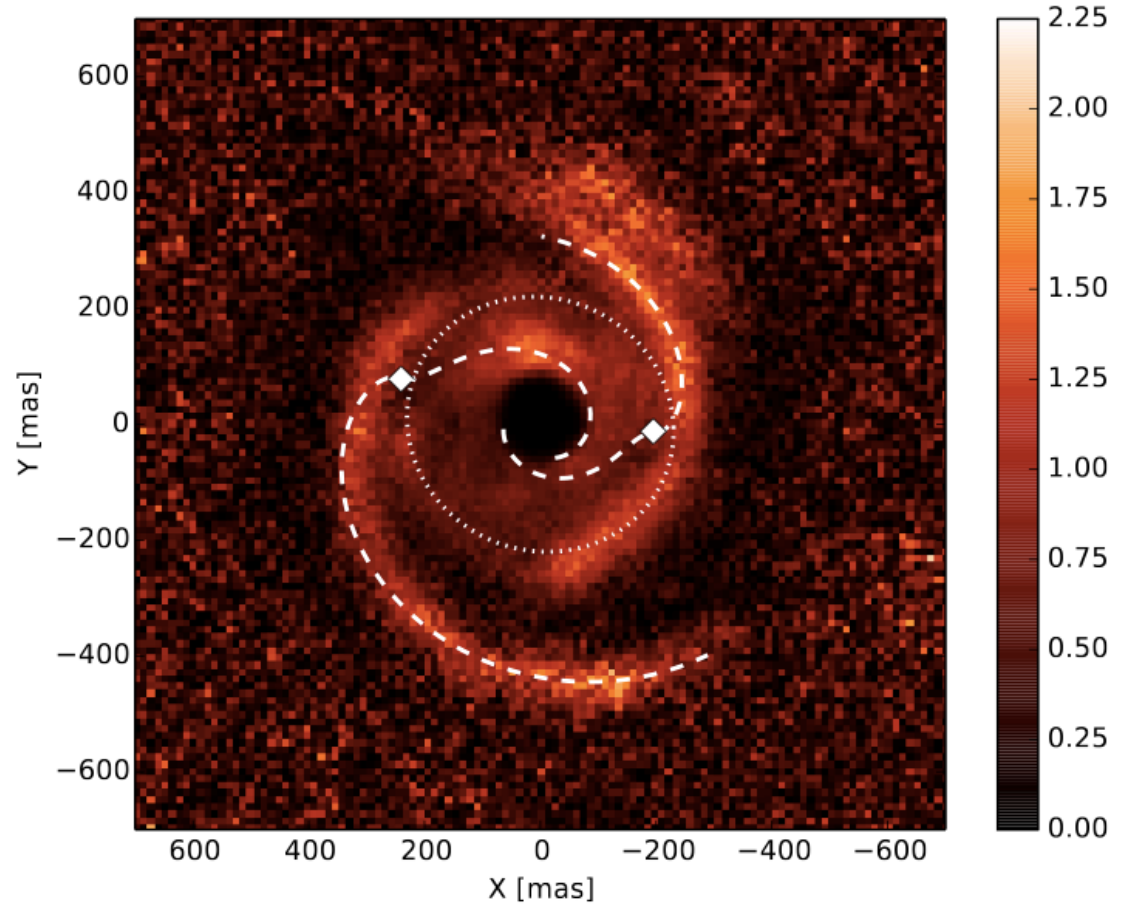


$$\theta(r) = \theta_c + \frac{\operatorname{sgn}(r - r_c)}{h_c} \times \left\{ \left(\frac{r}{r_c} \right)^{1+\beta} \left[\frac{1}{1+\beta} - \frac{1}{1-\alpha+\beta} \left(\frac{r}{r_c} \right)^{-\alpha} \right] - \left(\frac{1}{1+\beta} - \frac{1}{1-\alpha+\beta} \right) \right\},$$

Rafikov (2002)

Muto et al. (2012)

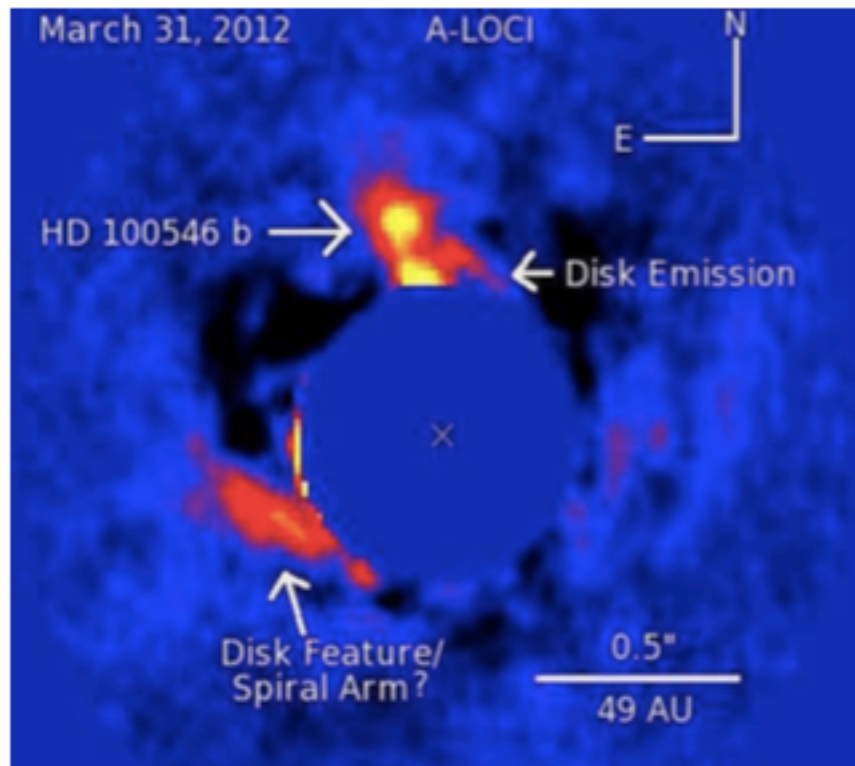
Spirals are **too wide**,
hotter (300K) than ambient gas (50K).



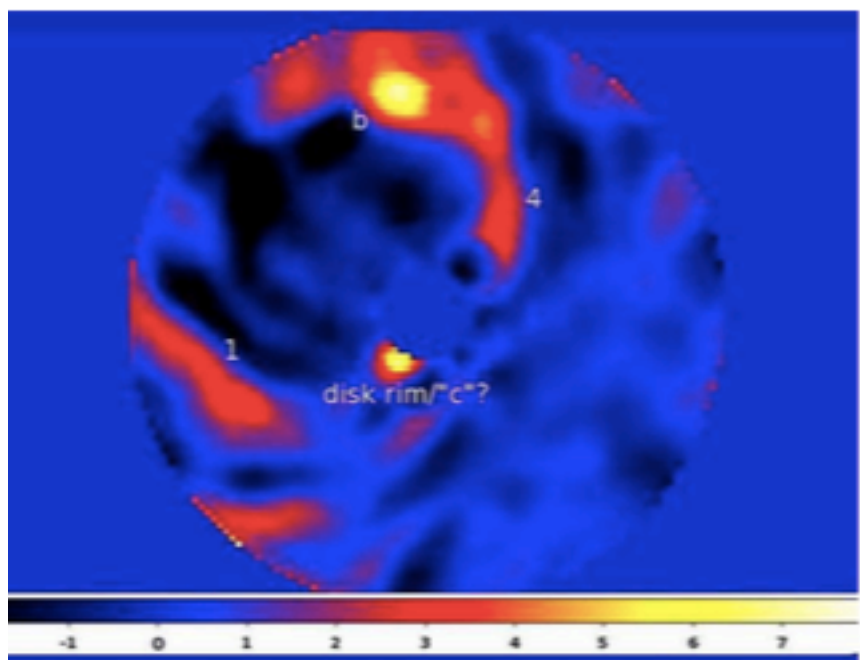
Benisty et al. (2015)

The strange case of thermal emission in HD 100546

L band ($\sim 3.5 \mu\text{m}$)

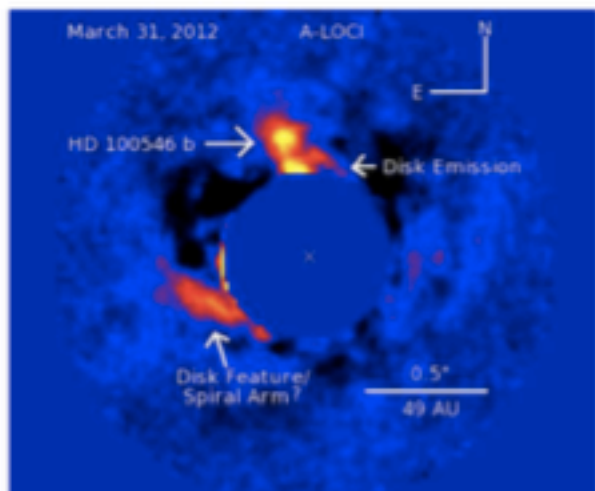


H band ($\sim 1.6 \mu\text{m}$)

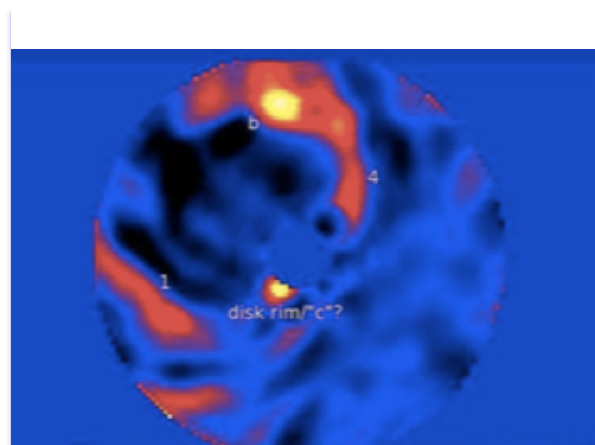


Currie et al. (2014), Currie et al. (2015)

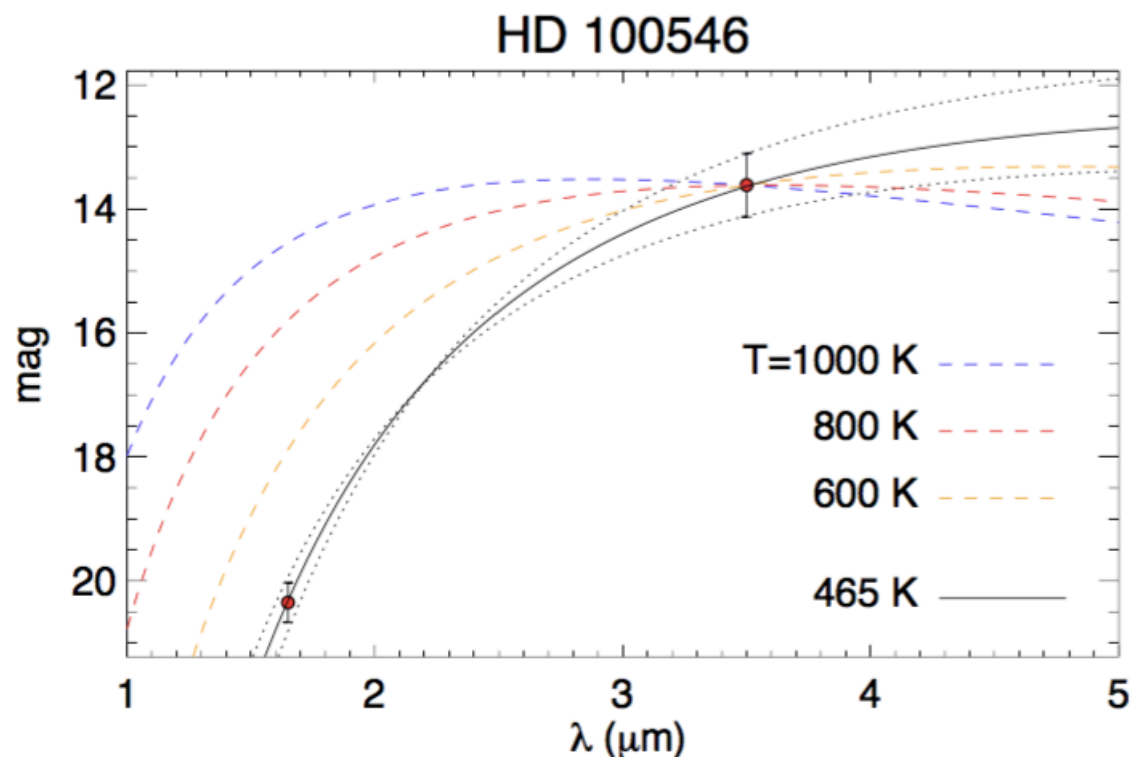
Pinning down the temperature



L band

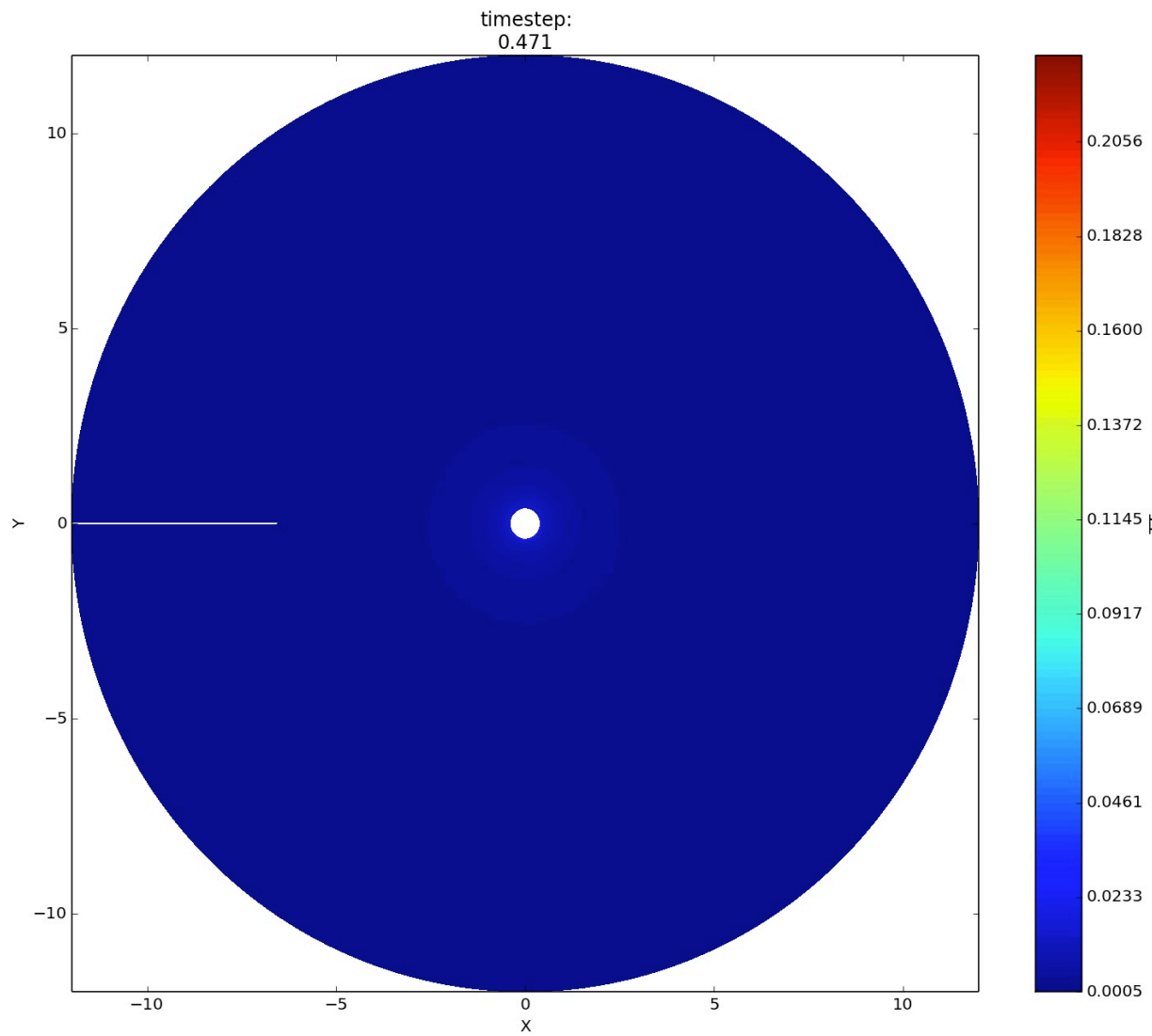


H band

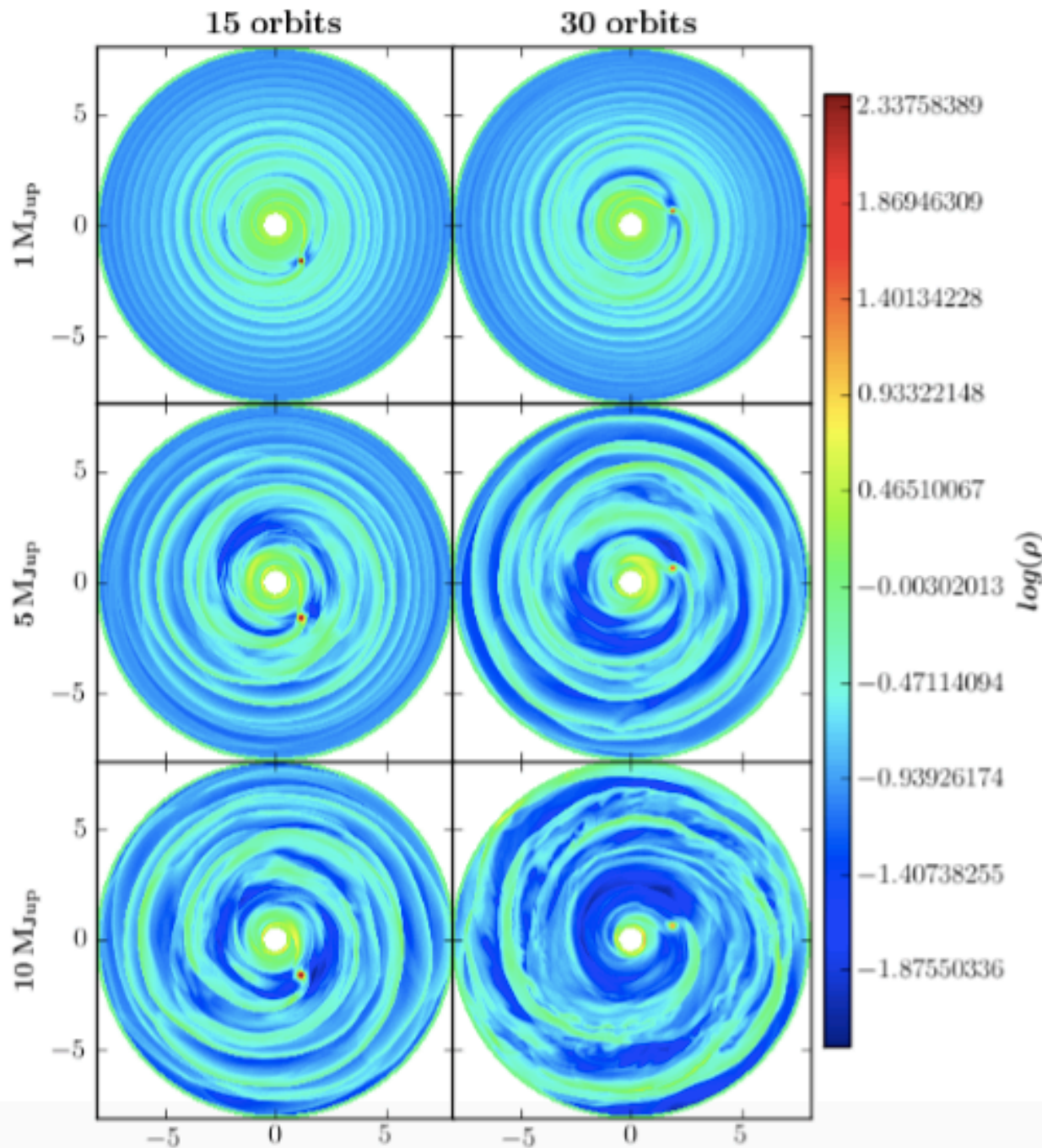


Lyra et al. (2016)

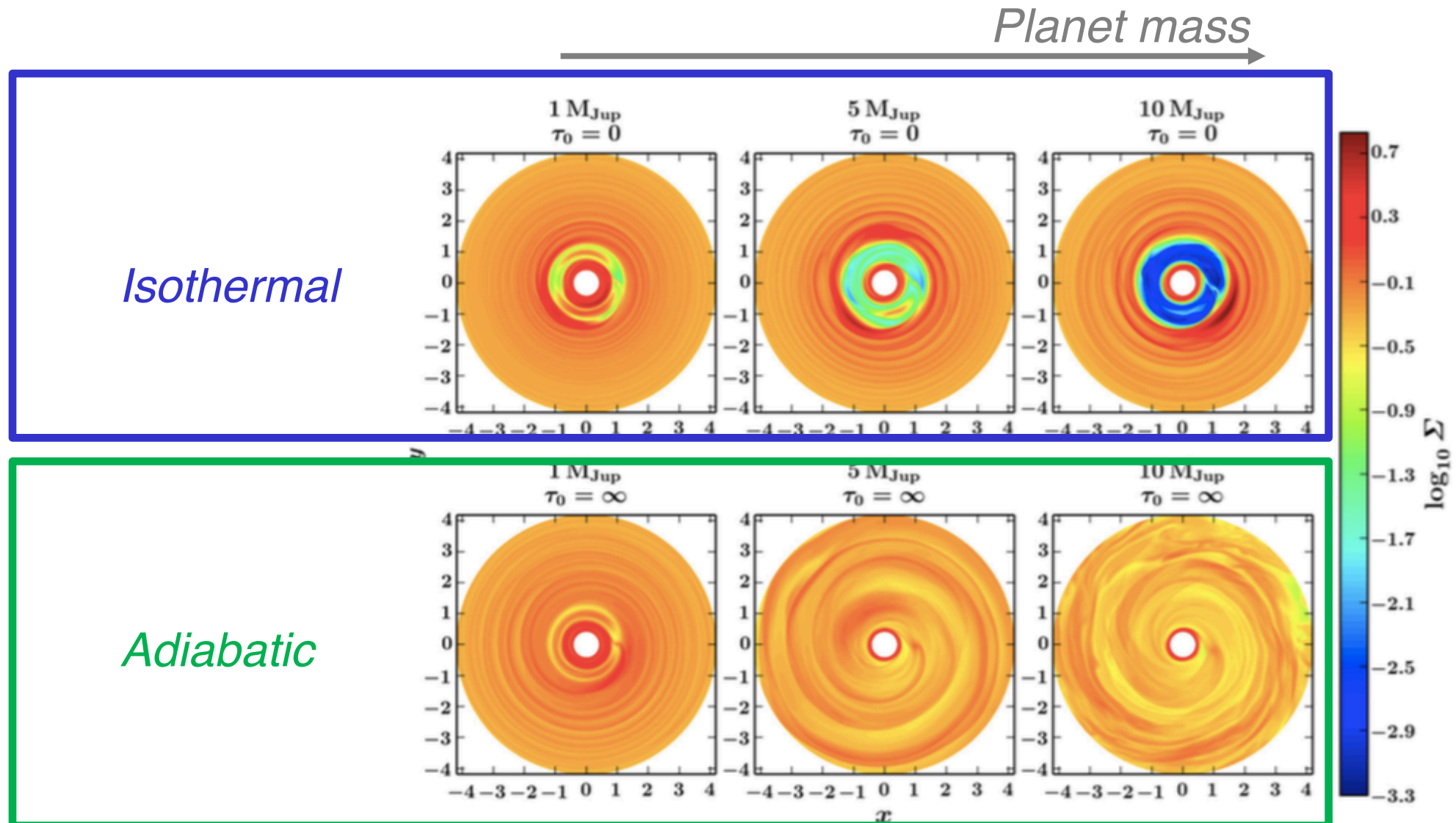
Planet-driven turbulence



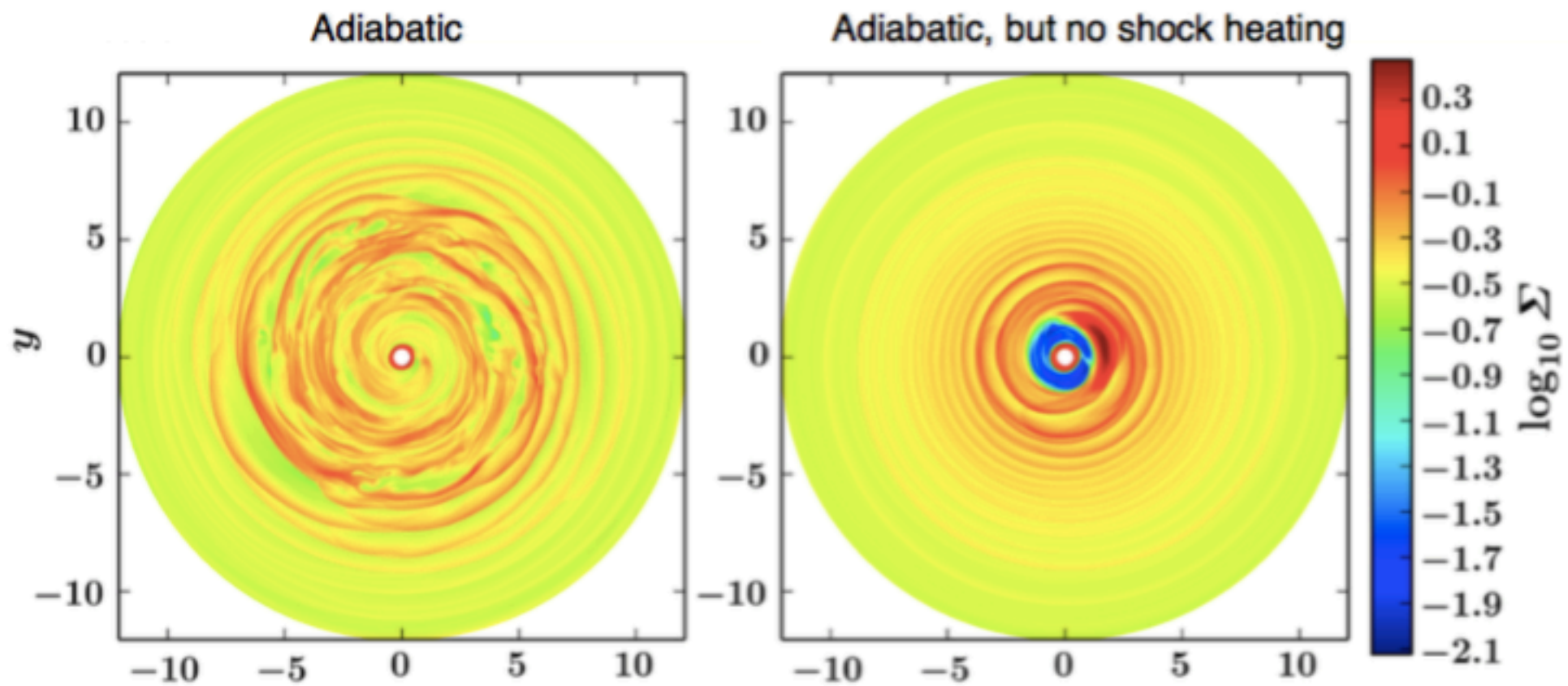
Some crazy turbulence showing up at high planet mass....



Turbulence in high-mass planets in adiabatic disks



The energy source: shock heating!



3D shocks: ascending bores and breaking waves

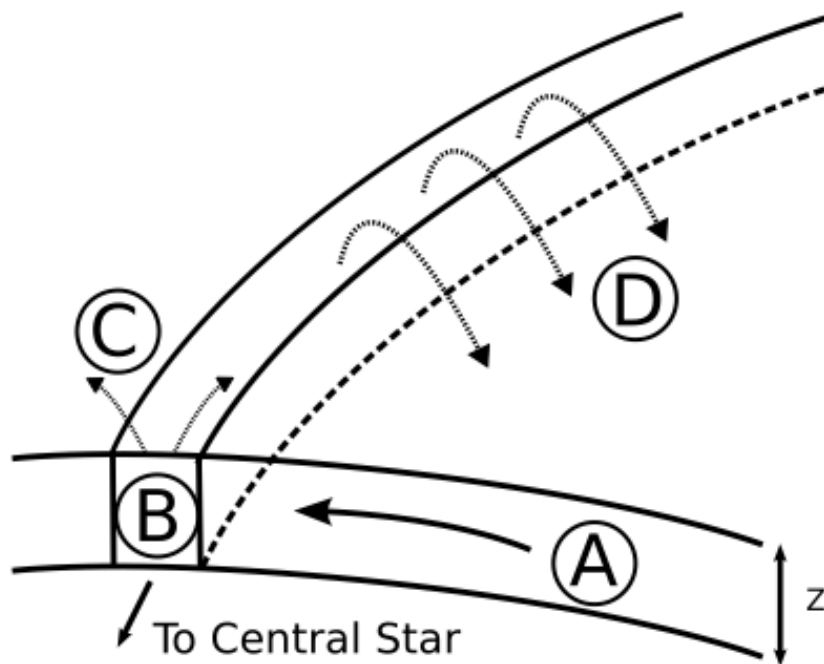
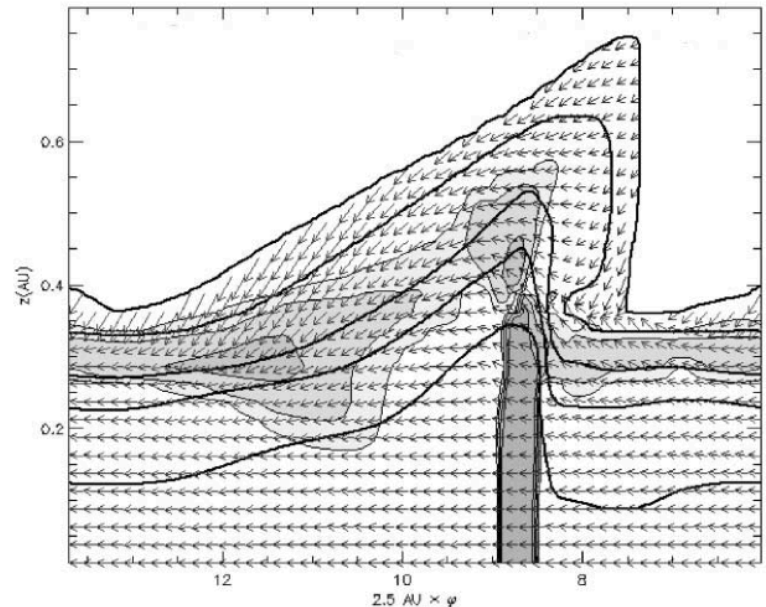
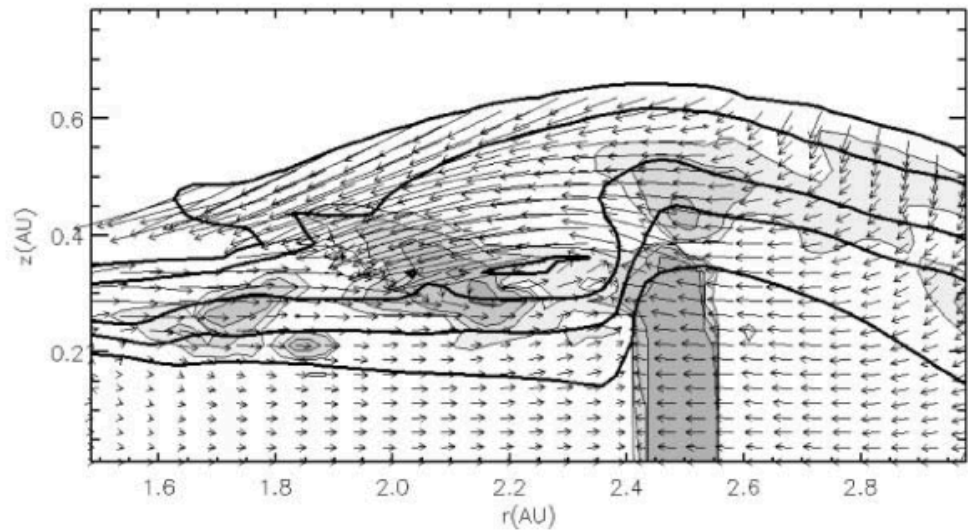


FIG. 2.—Cartoon depicting the gas flow in a shock bore in the frame of the spiral shock inside corotation. The gas in the preshock region flows into the spiral shock (A). The shock (B) causes the material to be out of vertical force balance and a rapid expansion results (C). Due to spiral streaming and the loss of pressure confinement, some of the gas will flow back over the spiral wave and break onto the disk in the preshock region at a radius inward from where it originated (D).



Radiative transfer approximation

$$T \frac{Ds}{Dt} = -c_V \frac{(T - T_{\text{ref}})}{t_{\text{cool}}} + \Gamma_{\text{sh}},$$

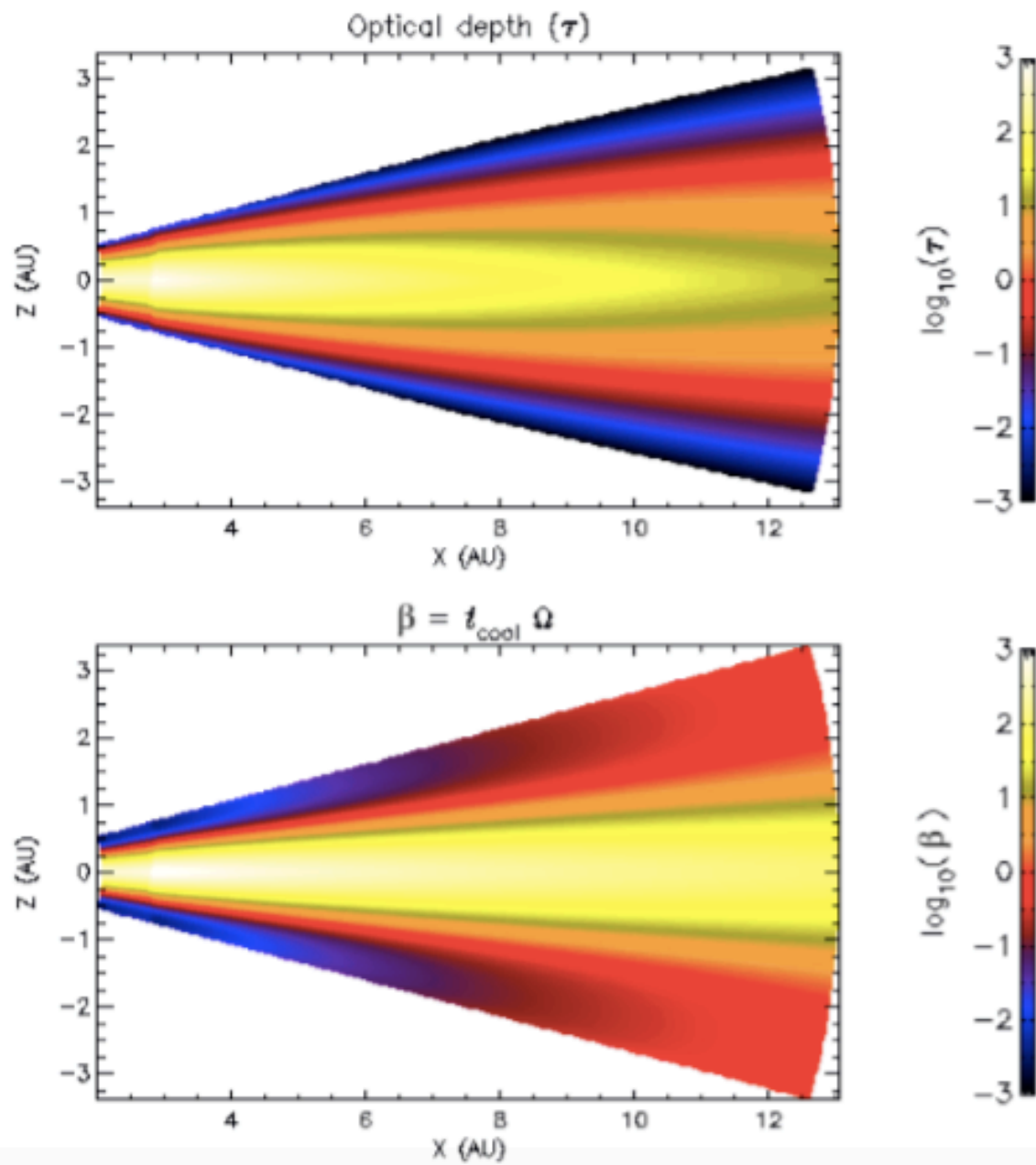
$$t_{\text{rad}} = E / \dot{E}$$

$$\dot{E} = \nabla \cdot F$$

$$t_{\text{cool}} \equiv \frac{\int E dV}{\int F \hat{n} \cdot dA}.$$

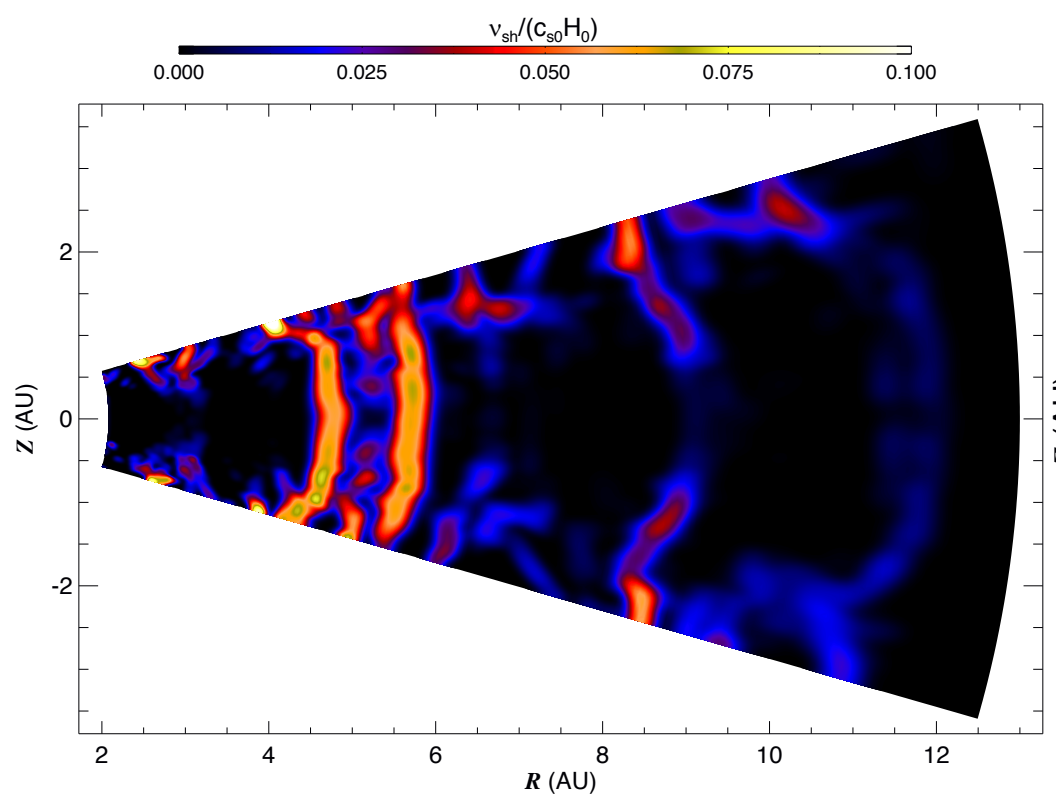
$$t_{\text{cool}} = \frac{c_V \rho H \tau_{\text{eff}}}{3\sigma T^3}.$$

$$\tau_{\text{eff}} = \frac{3\tau}{8} + \frac{\sqrt{3}}{4} + \frac{1}{4\tau}.$$

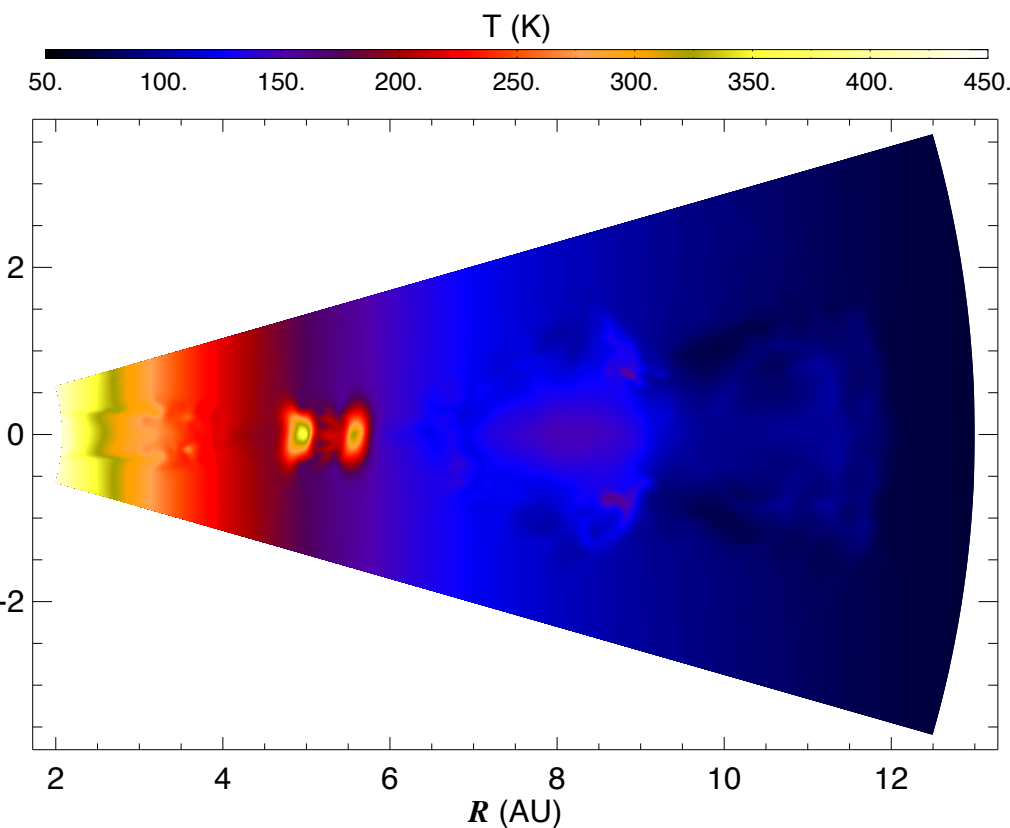


3D: Shock bores

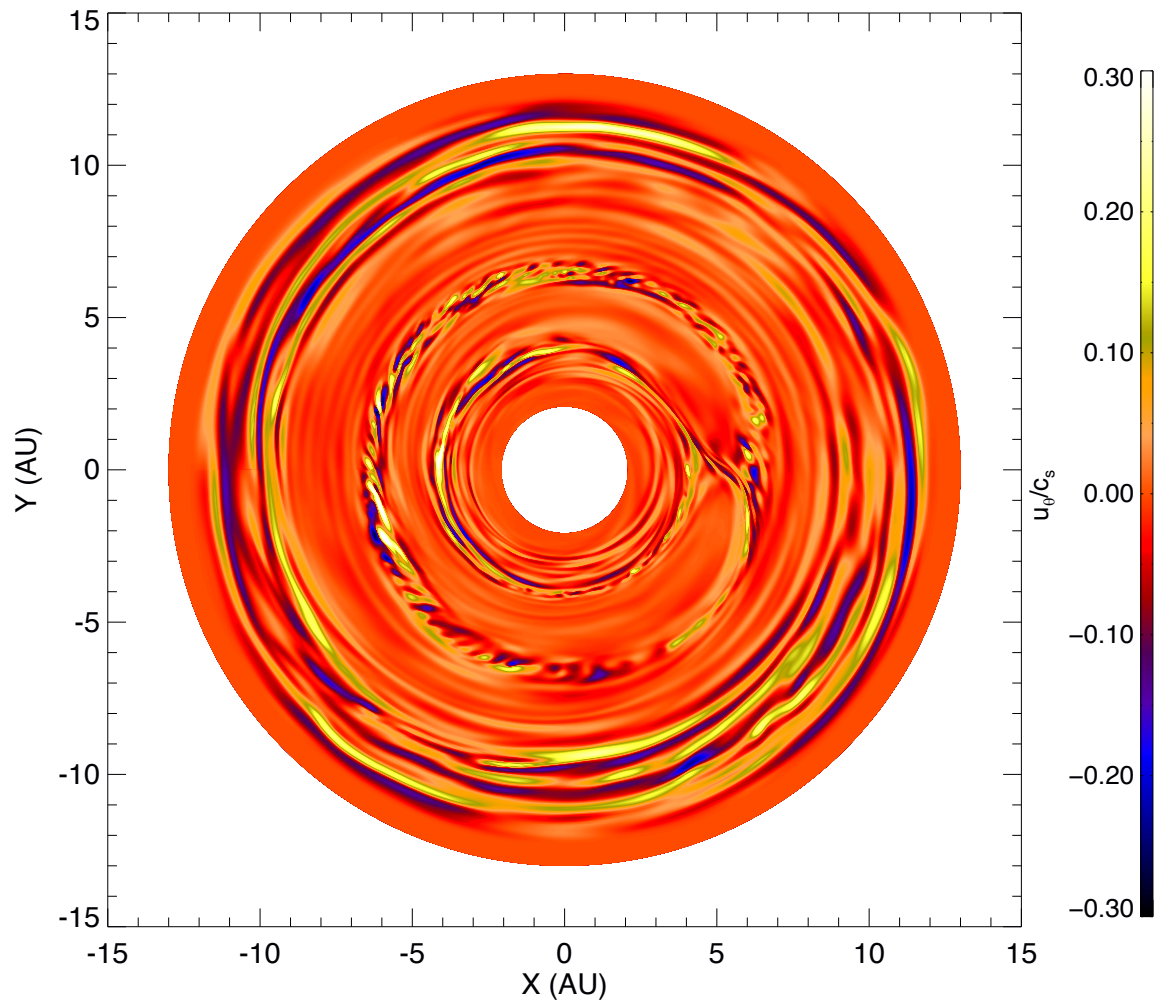
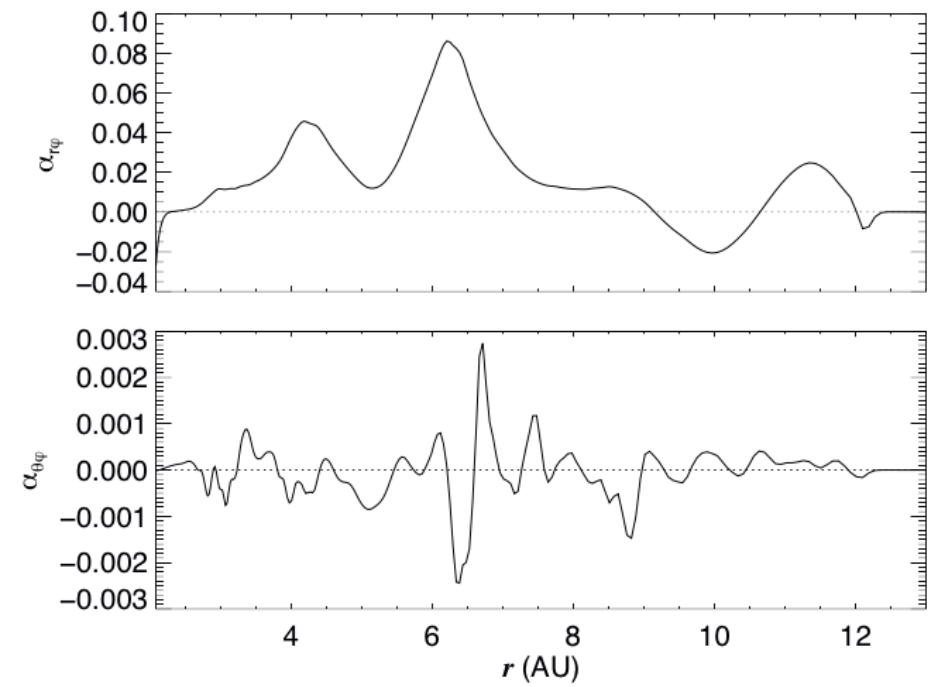
Shocks (velocity convergence)



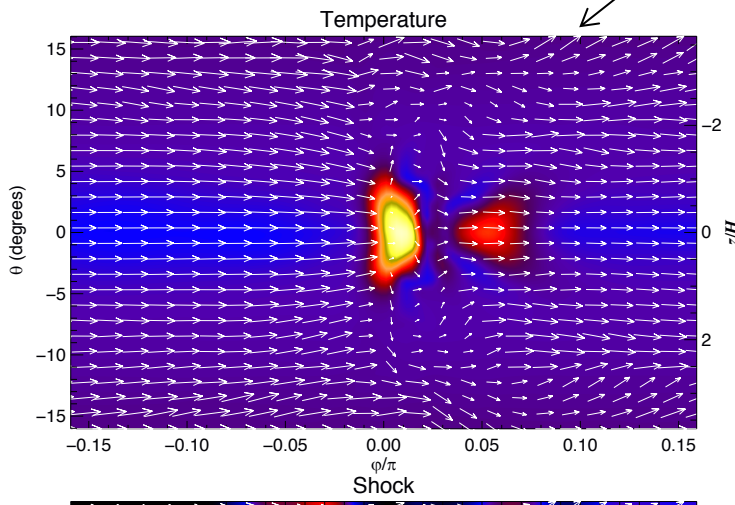
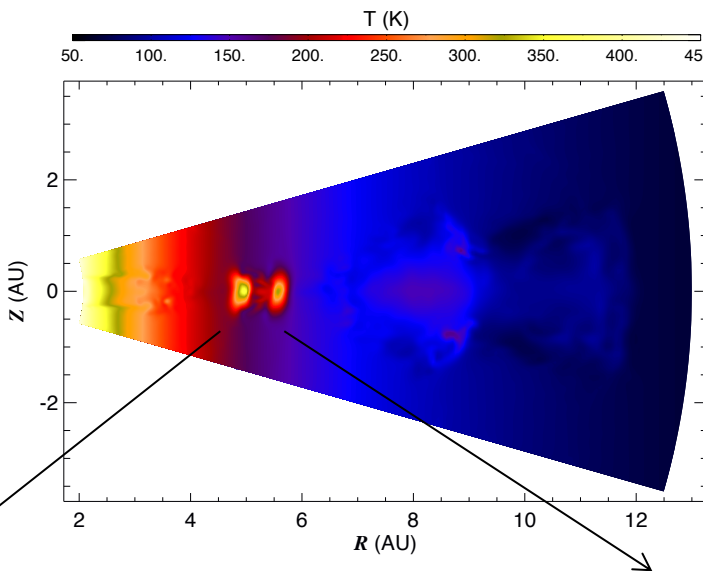
Temperature



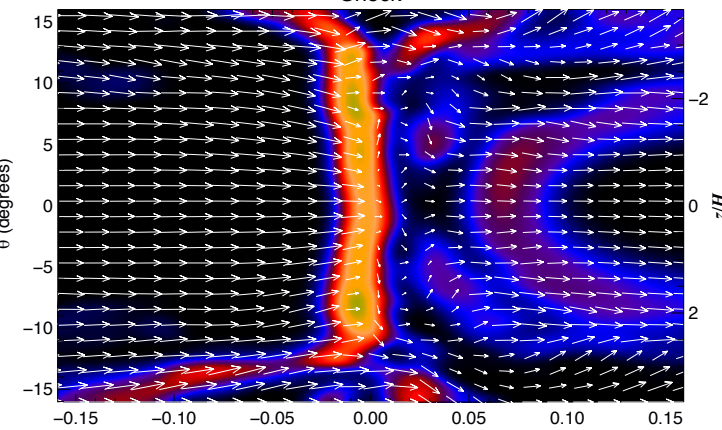
Prediction for spectroscopy: Turbulent surf



3D shocks: bores and breaking waves

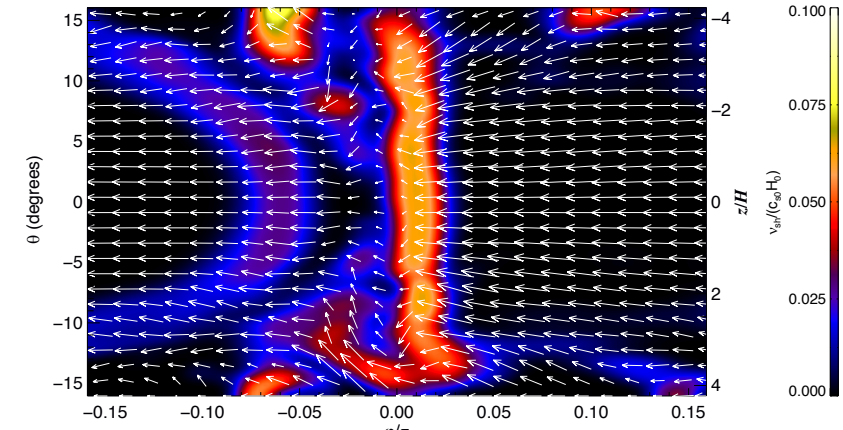
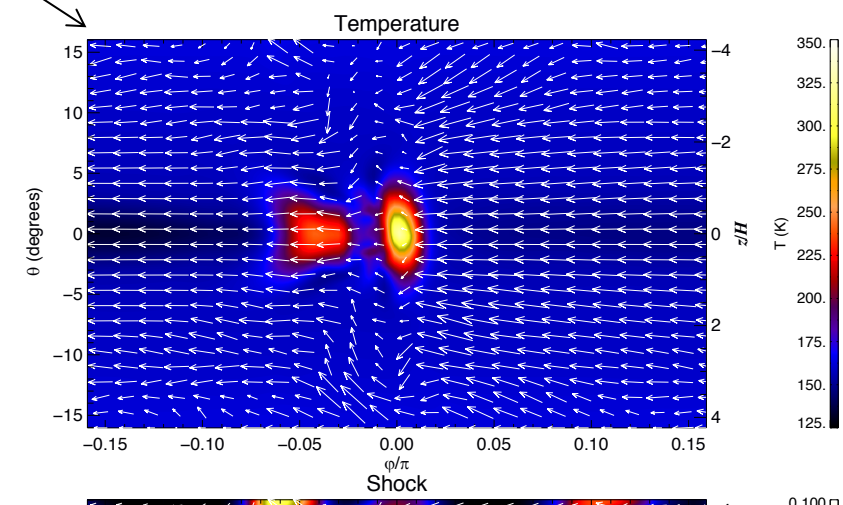


Temperature



Div u
(shock)

Lyra et al. (2016)



Shock heating and opacities

$$\mathcal{H}_{\text{sh}} = \rho \nu_{\text{sh}} (\nabla \cdot \mathbf{u})^2$$

$$\nu_{\text{sh}} = c_{\text{sh}} \left\langle \max_3 [(-\nabla \cdot \mathbf{u})^+] \right\rangle [\min(\Delta x)]^2$$

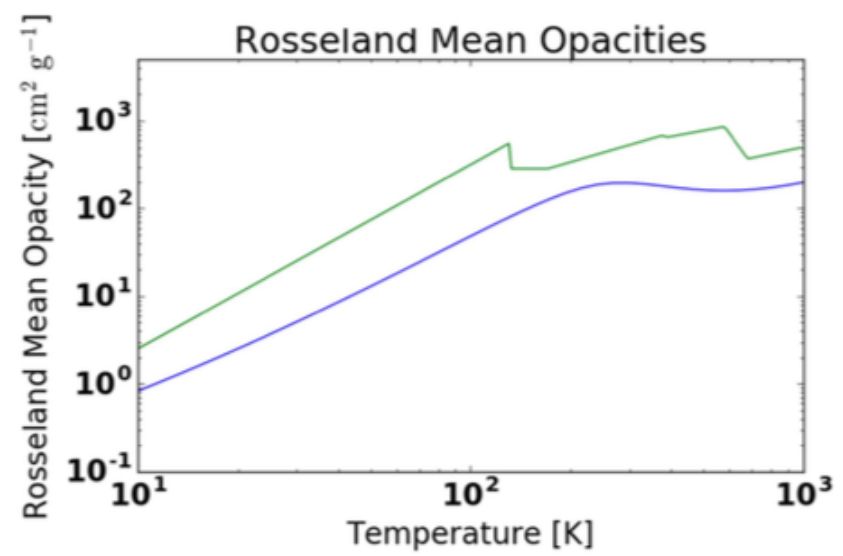
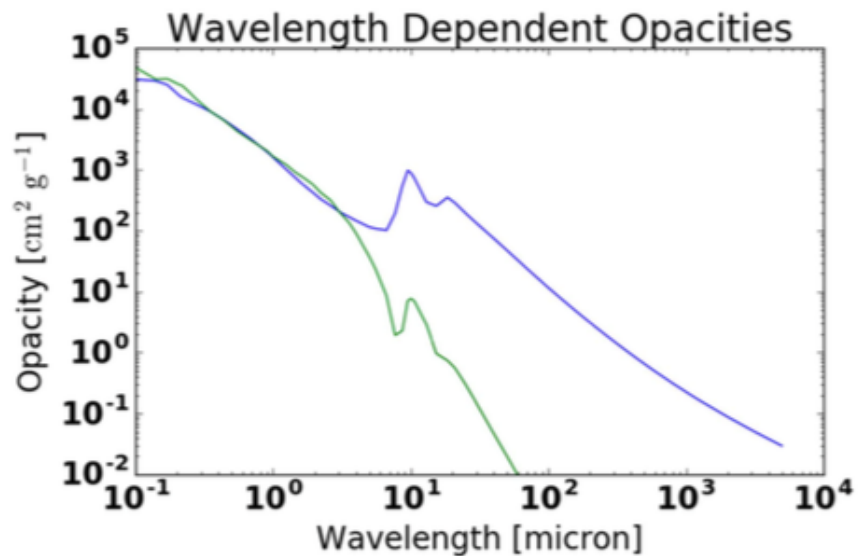
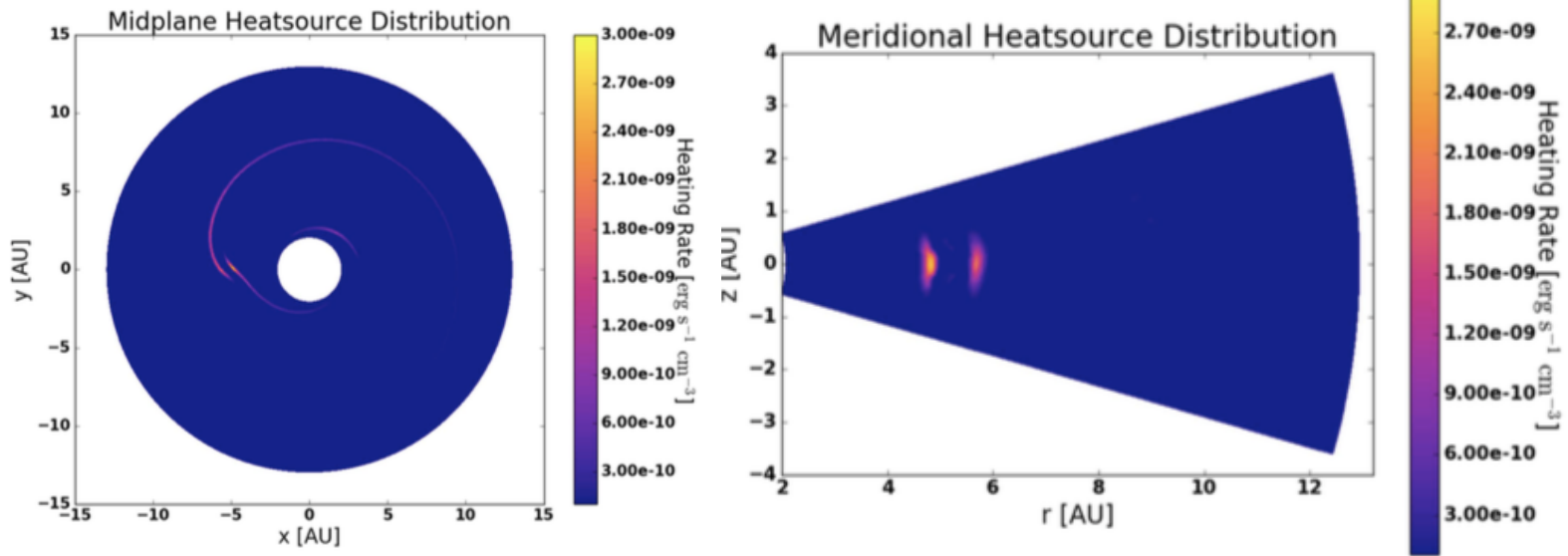
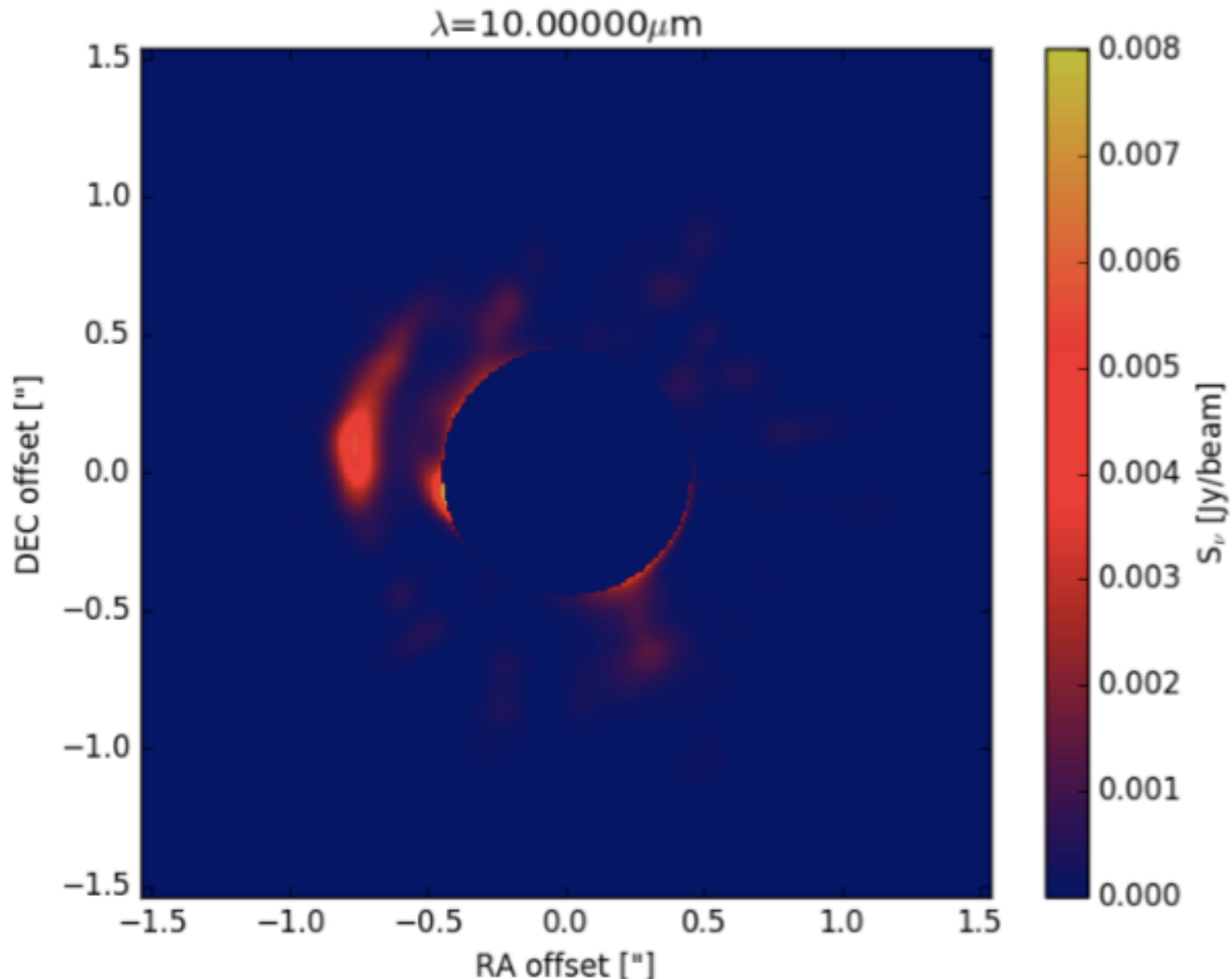
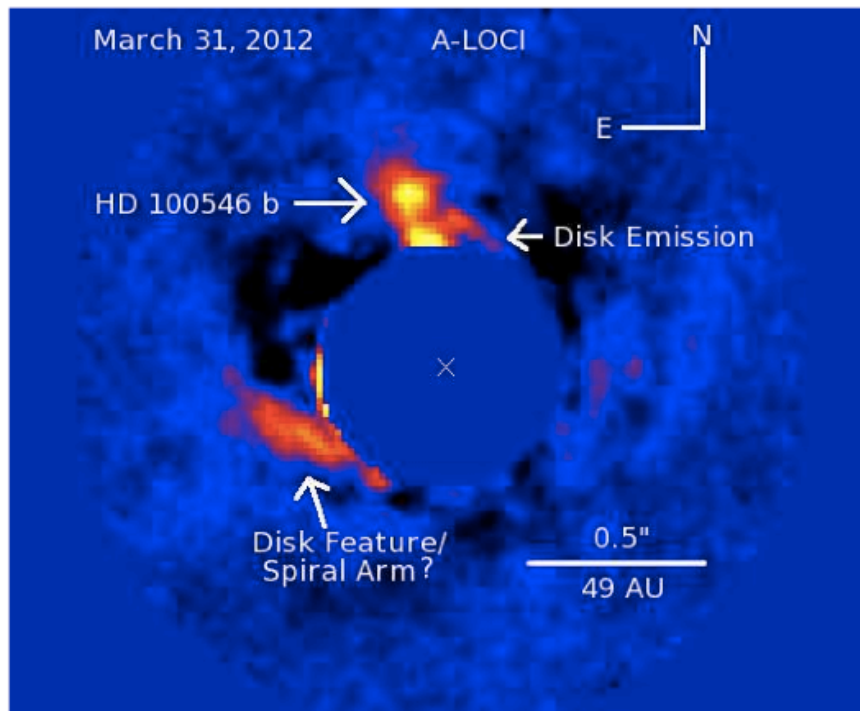


Figure 1. Wavelength-dependent opacities from Preibisch et al. (1993), including the absorption (top, blue) and scattering (top, green) opacities, input into RADMC-3D. The calculated Rosseland mean opacities (bottom, blue) match the Rosseland mean of Bell et al. (1997). The piece-wise Rosseland Mean opacity based on D'Angelo et al. (2003) and implemented in the Pencil Code (bottom, green) only varies by at most a factor of two from the calculation.

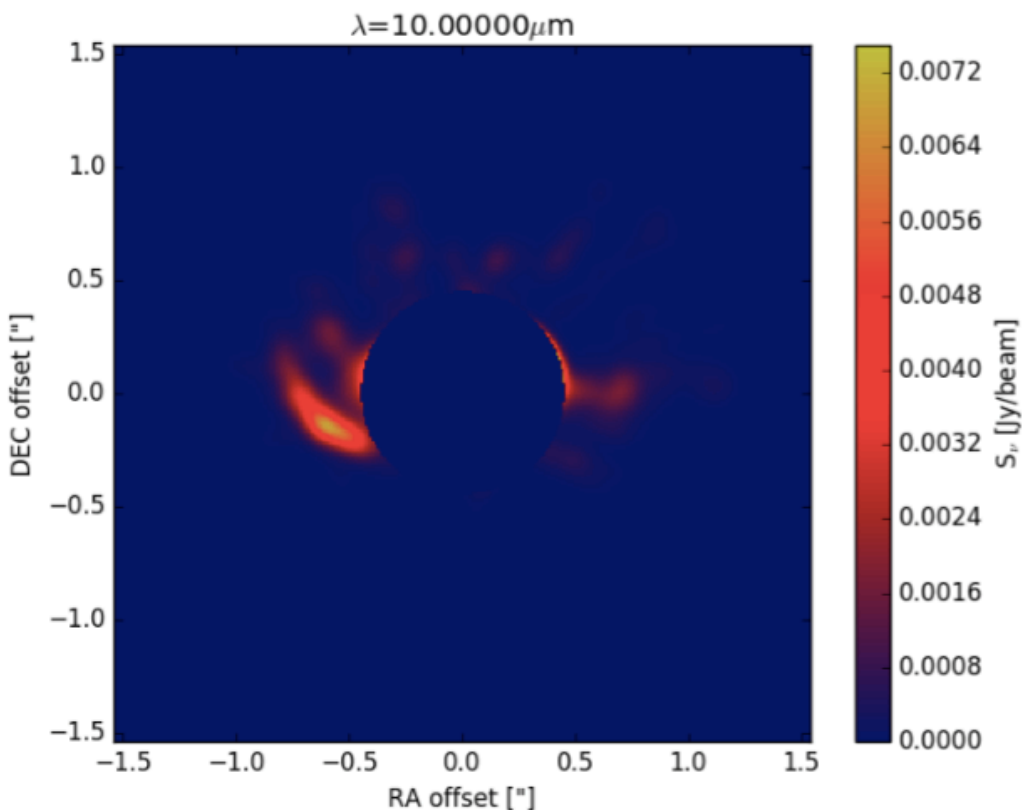
Synthetic image by RADM3D and shock heating



Observation vs Synthetic Image

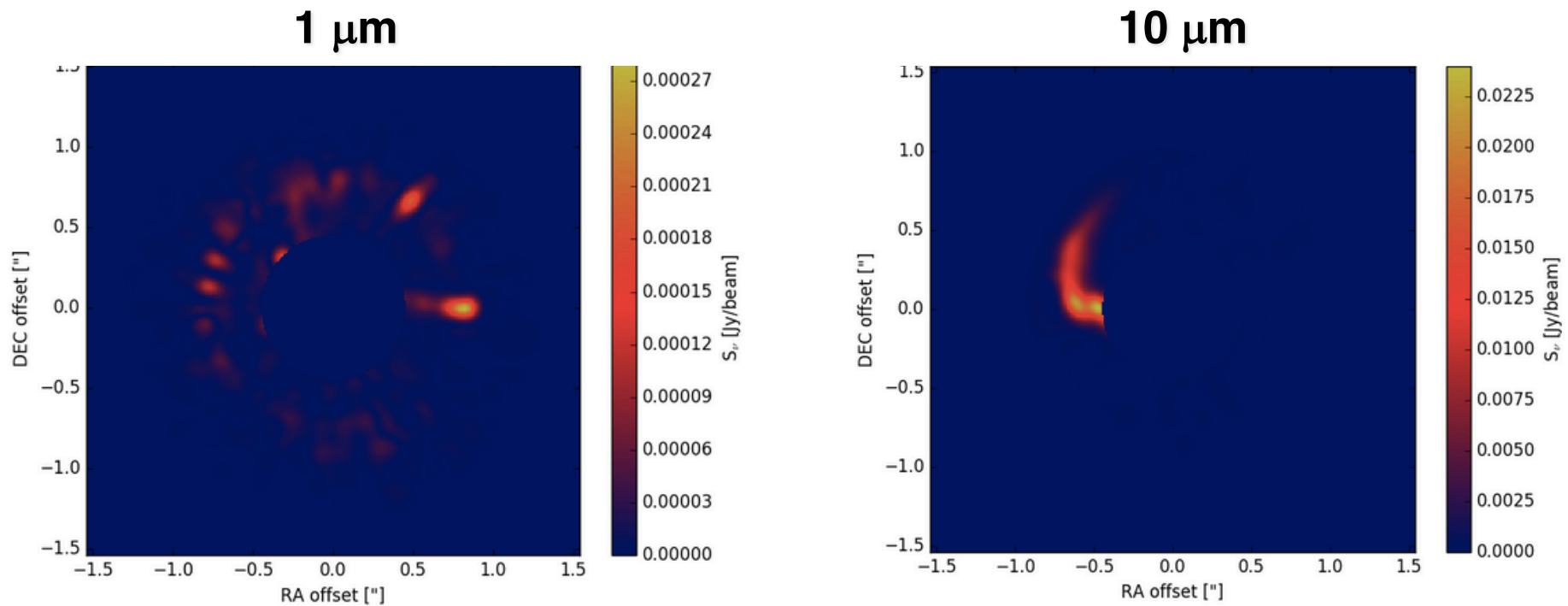


Currie et al. (2015)



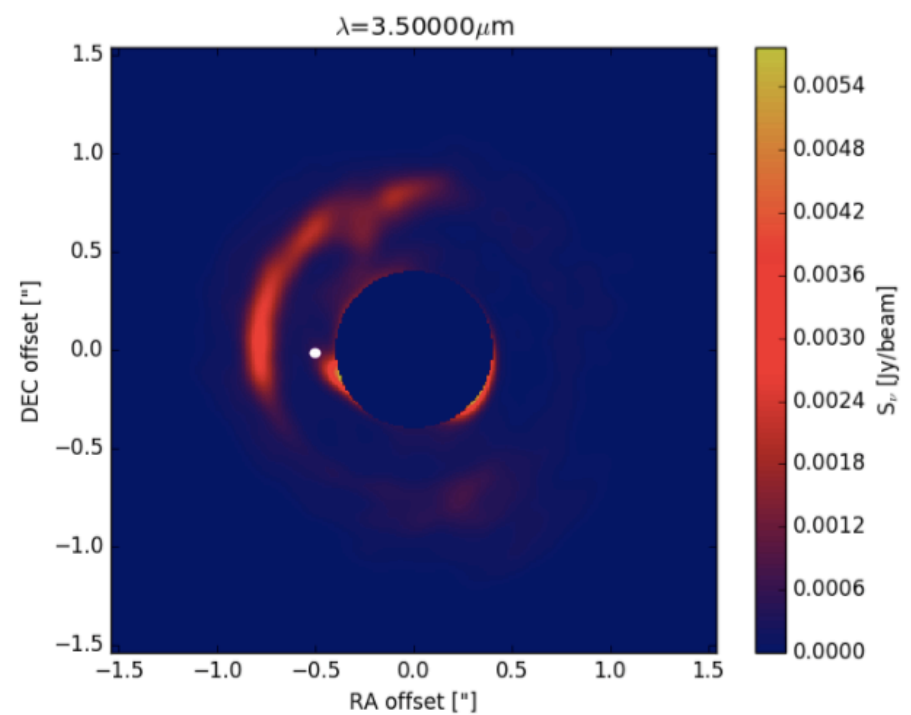
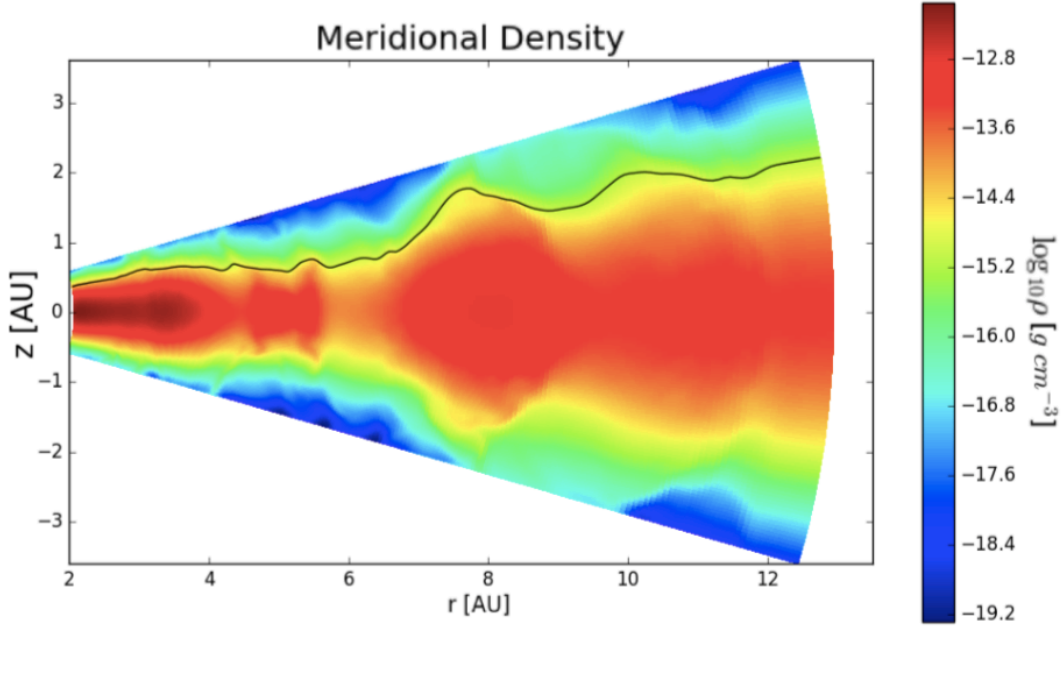
Hord et al. (2017)

Effect of shocks alone



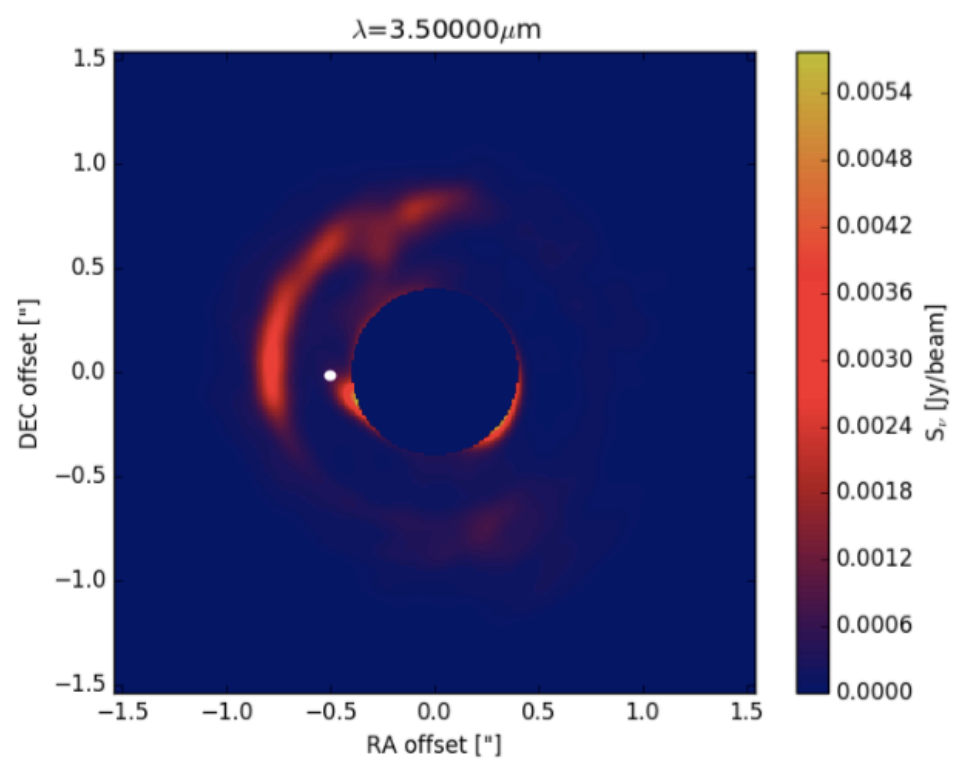
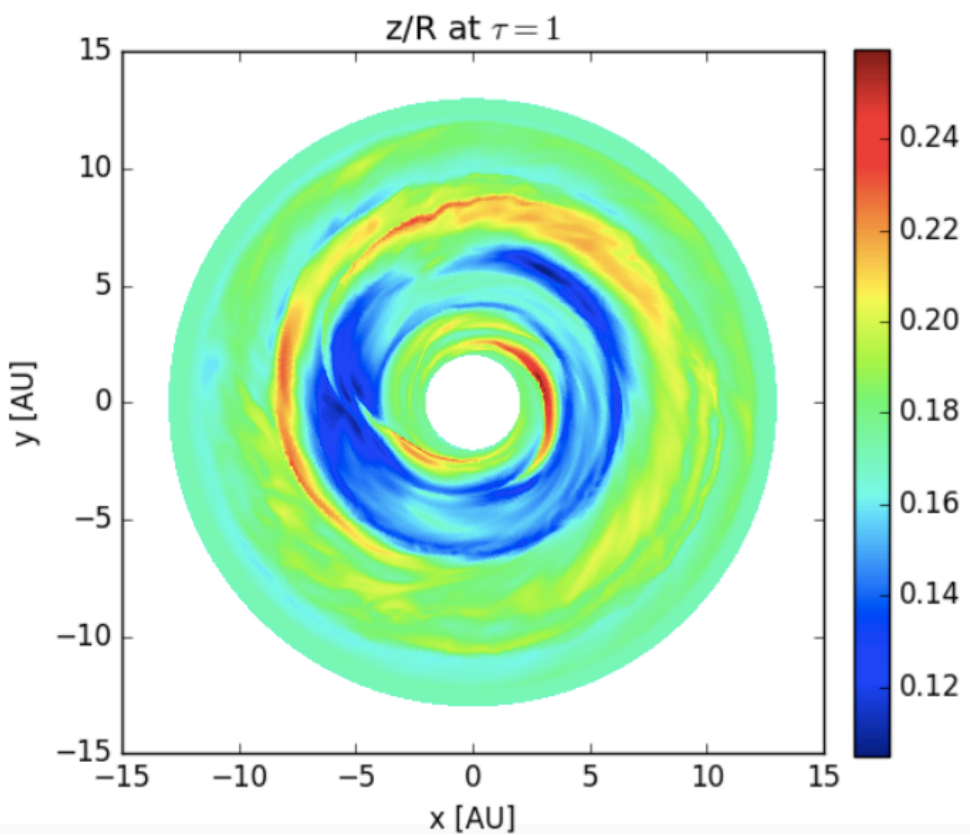
Hord et al. (2017)

Scattering – A puffed up outer gap



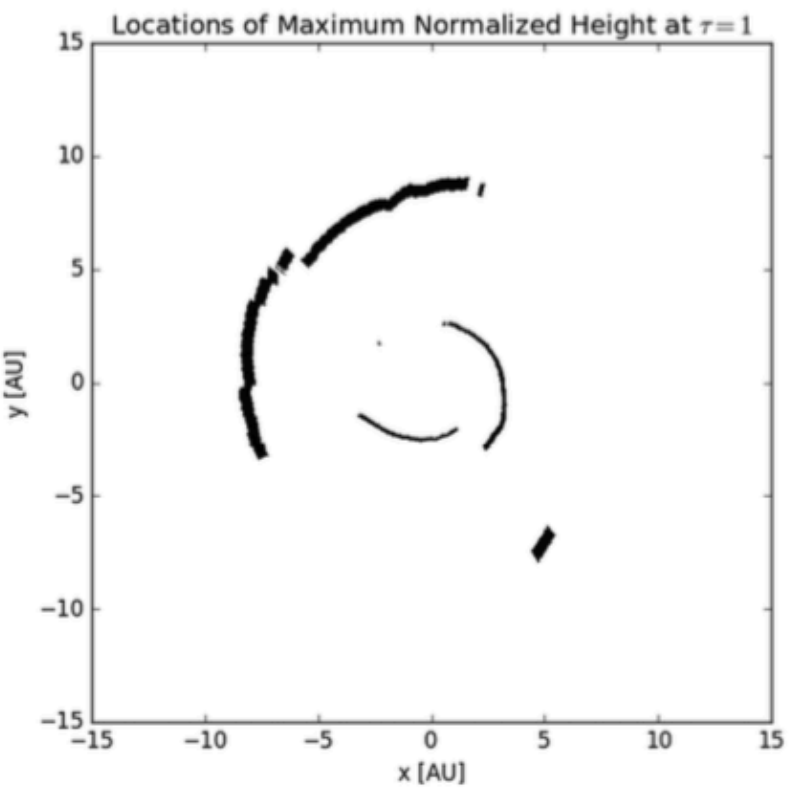
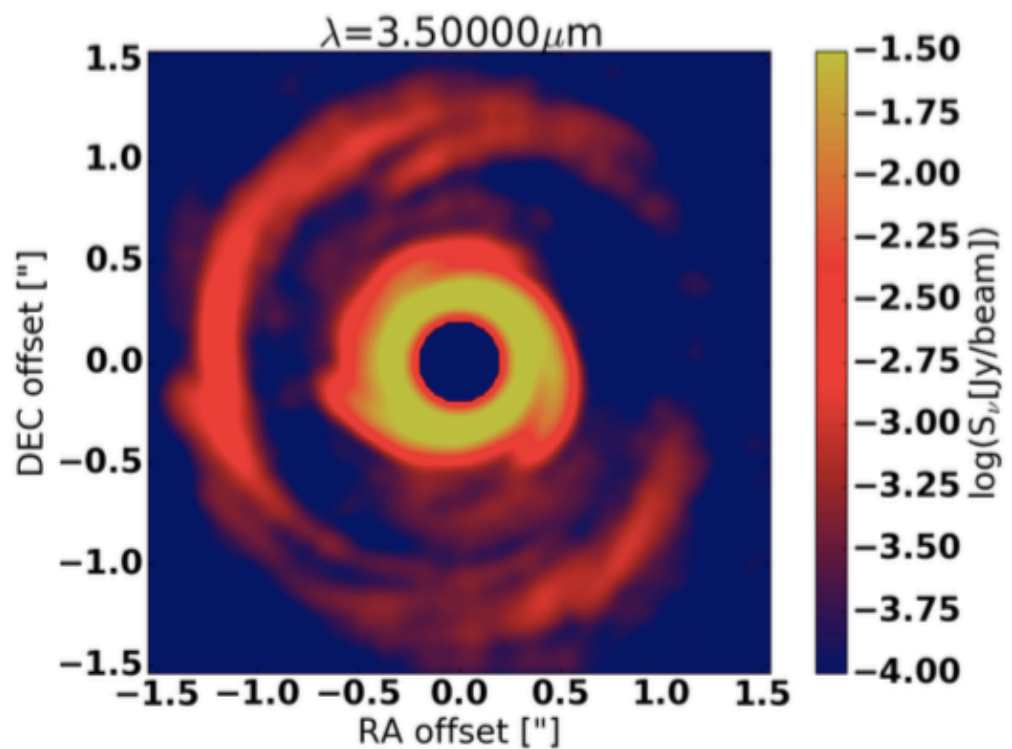
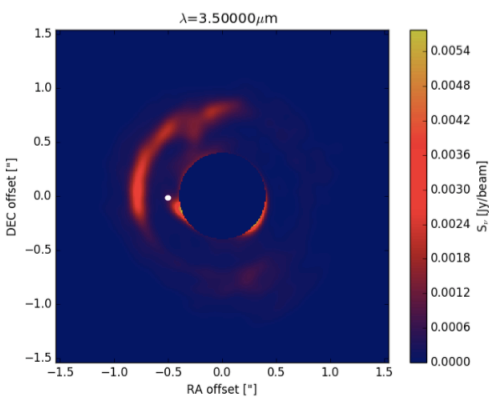
Hord et al. (2017)

Scattering



Hord et al. (2017)

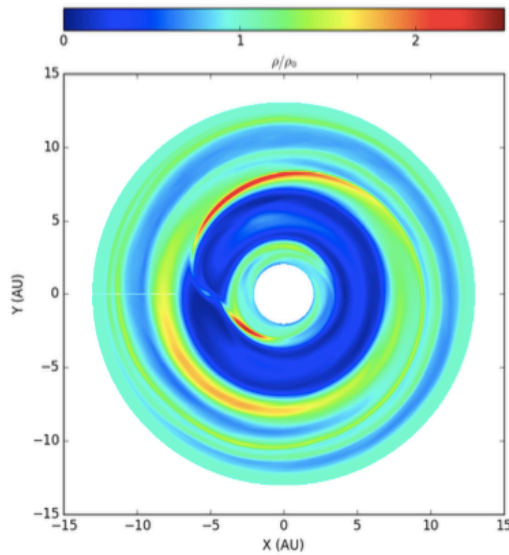
We see what is not in the
shadow of the inner disk spirals



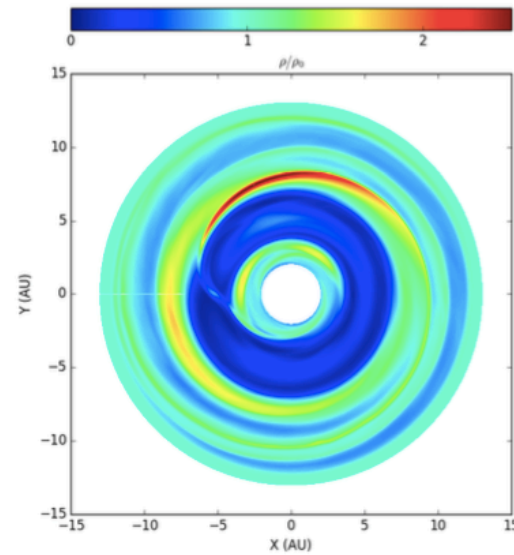
Hord et al. (2017)

The pattern is stationary

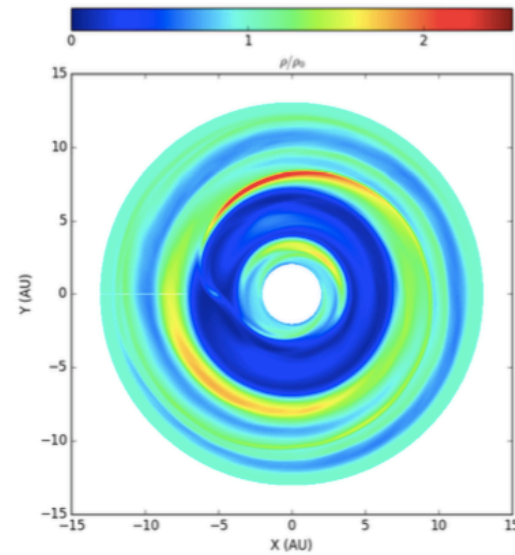
$T = 39$ orbits



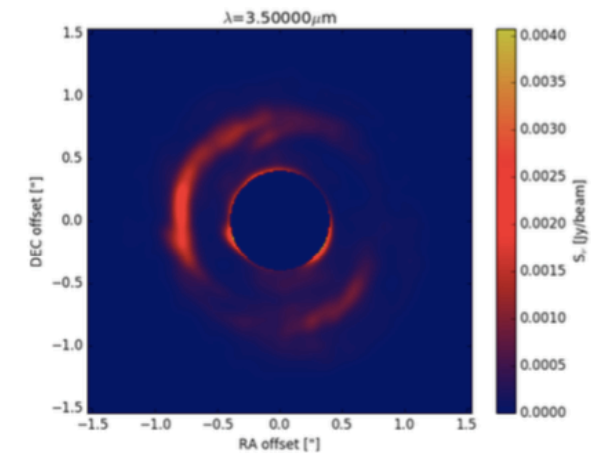
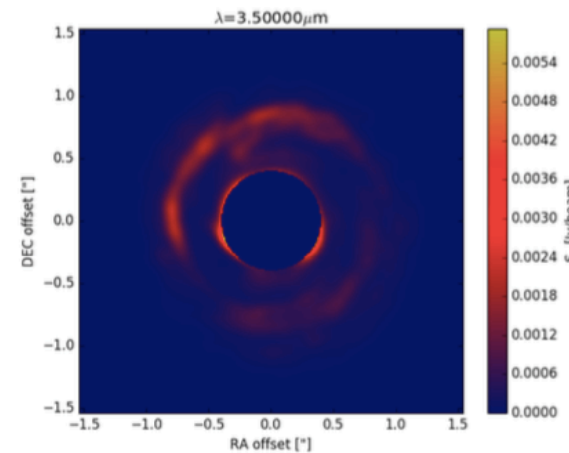
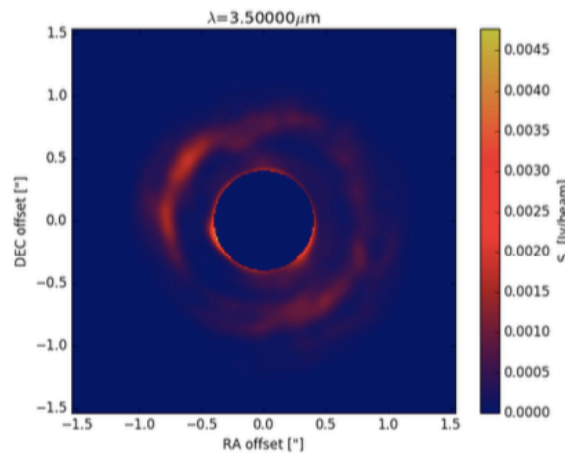
$T = 40$ orbits



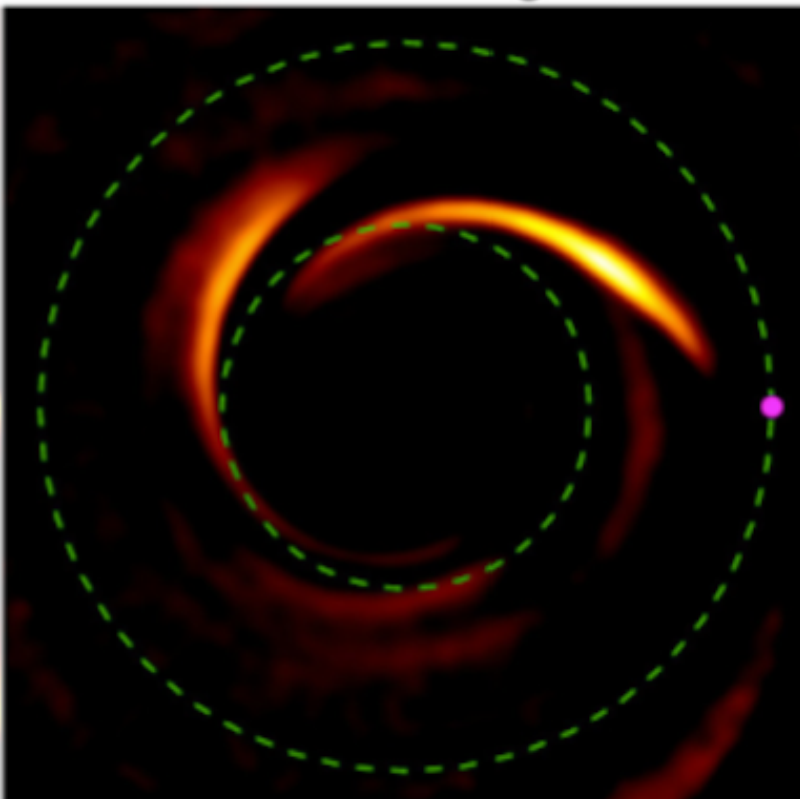
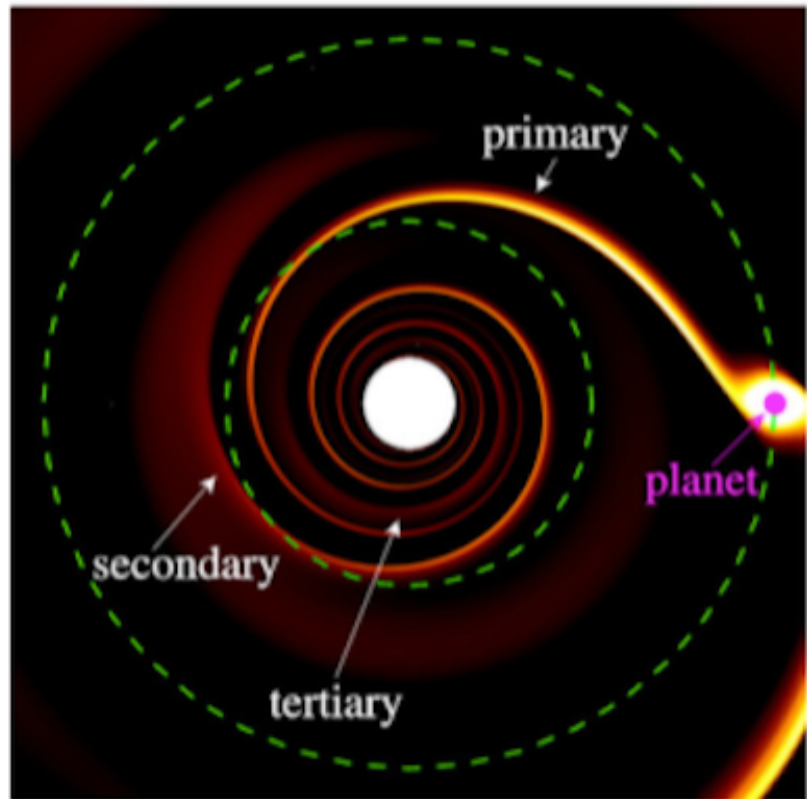
$T = 41$ orbits



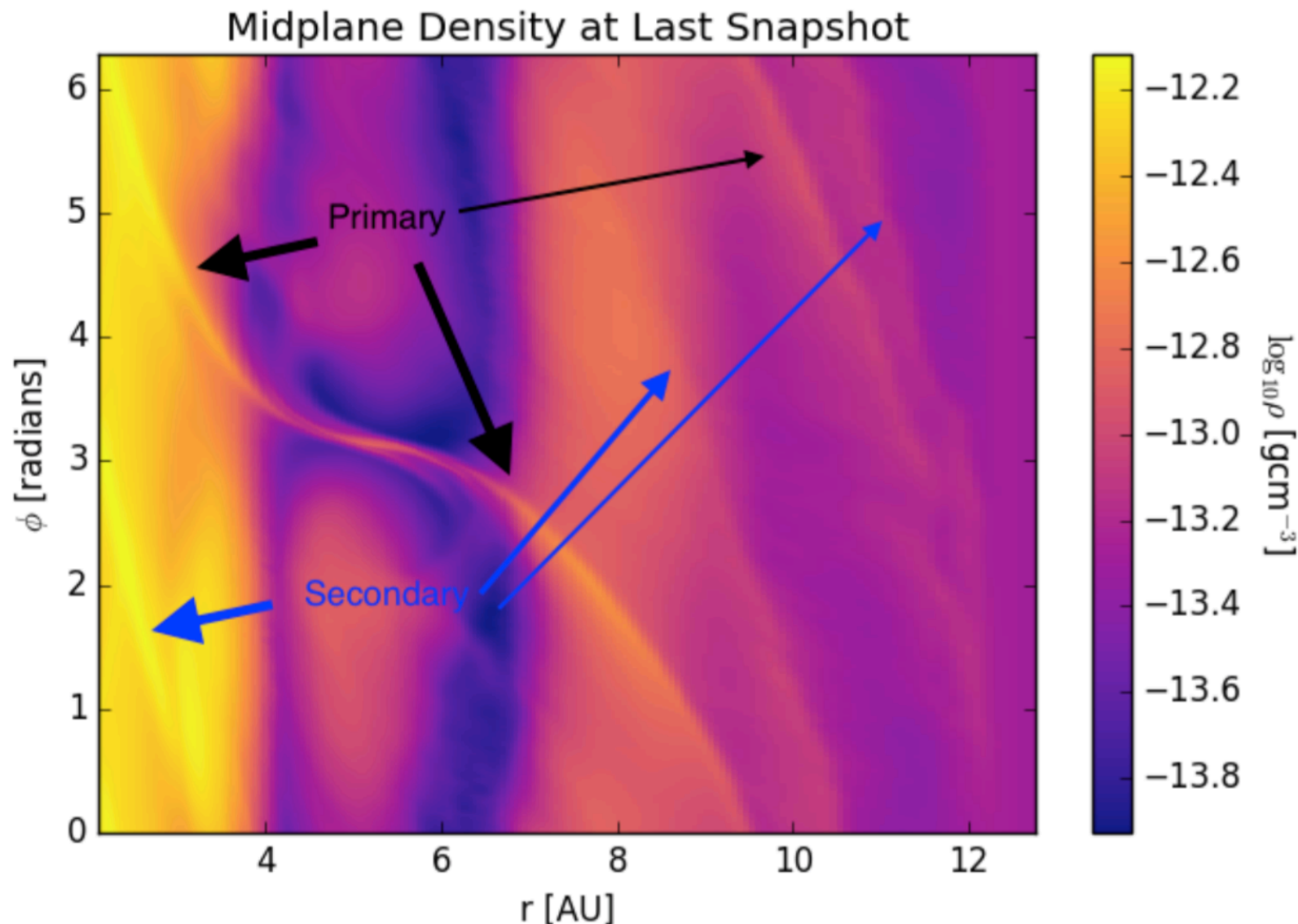
Intensity



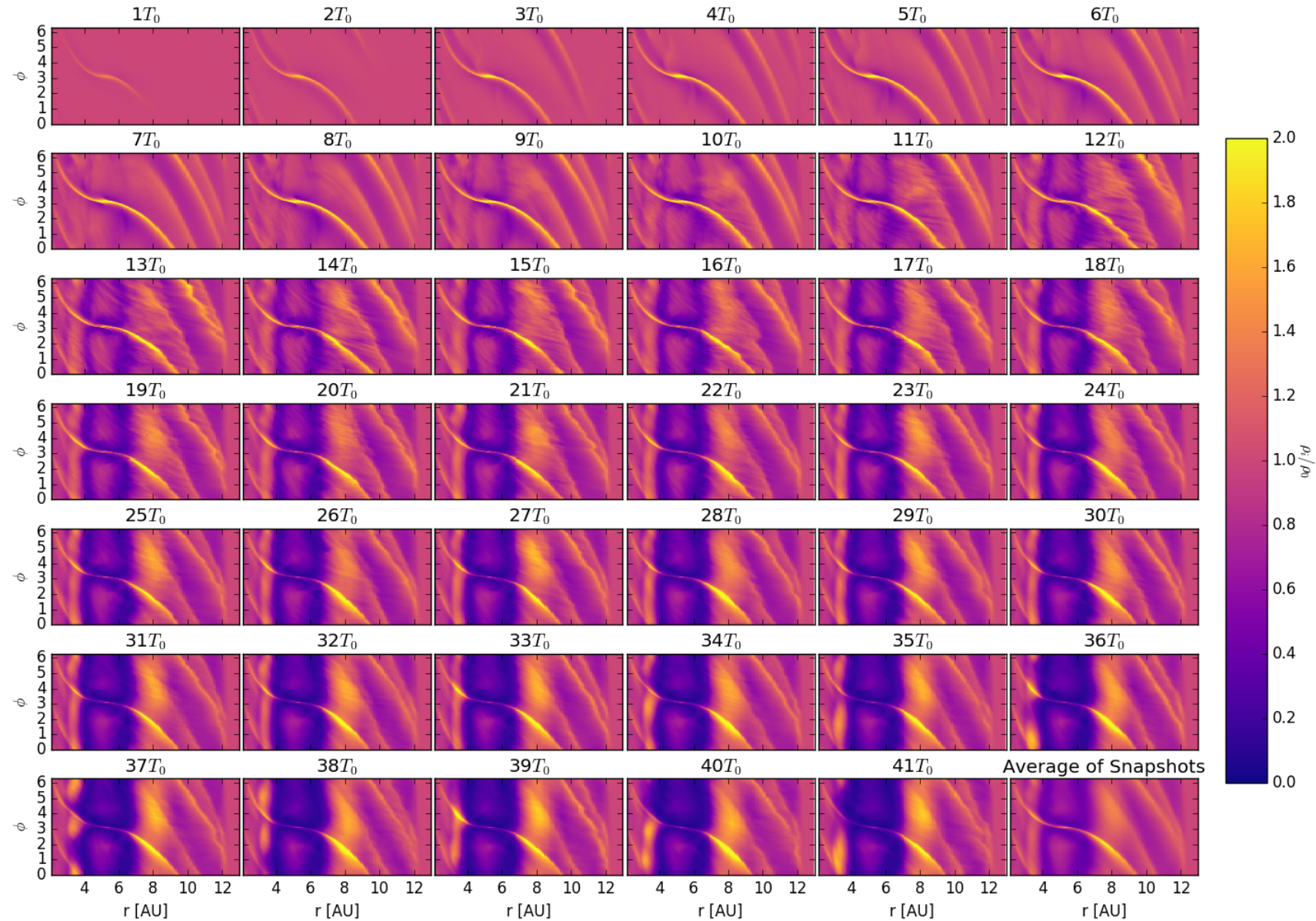
Primary and Secondary spiral arms



Primary and Secondary spiral arms

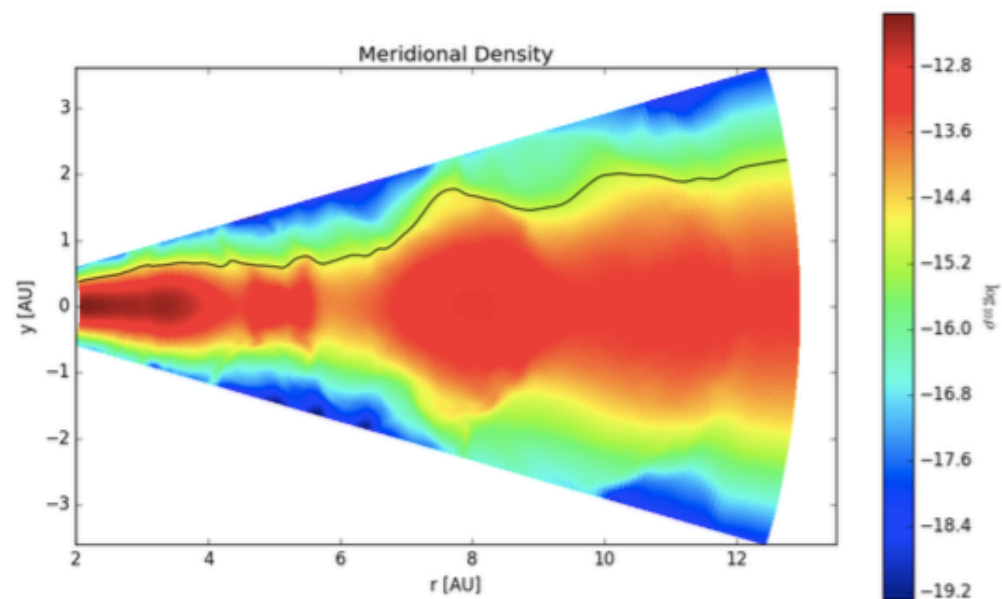
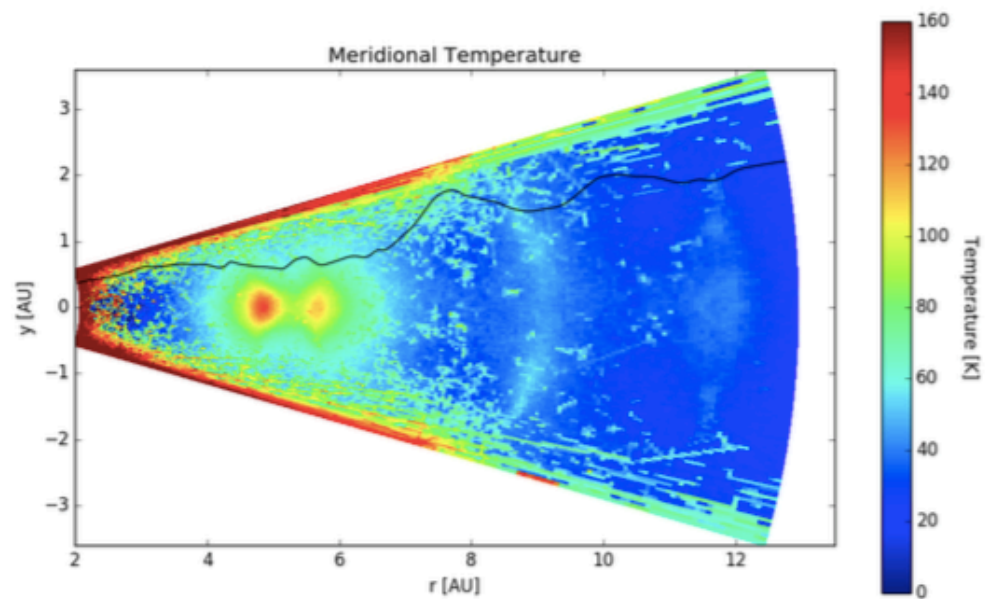


The raised feature has its origins in a secondary spiral arm



Conclusions

- 3D radiation-hydro models give results widely different than 2D isothermal
- Planet-induced shocks modify disk structure
- Hot lobes near high-mass planets in high resolution
- Planets puff up their outer gaps – visible in scattered light



Conclusions

- 3D radiation-hydro models give results widely different than 2D isothermal
- Planet-induced shocks modify disk structure
- Hot lobes near high-mass planets in high resolution
- Planets puff up their outer gaps – visible in scattered light

